

109.01

Engineering Geology 工程地質

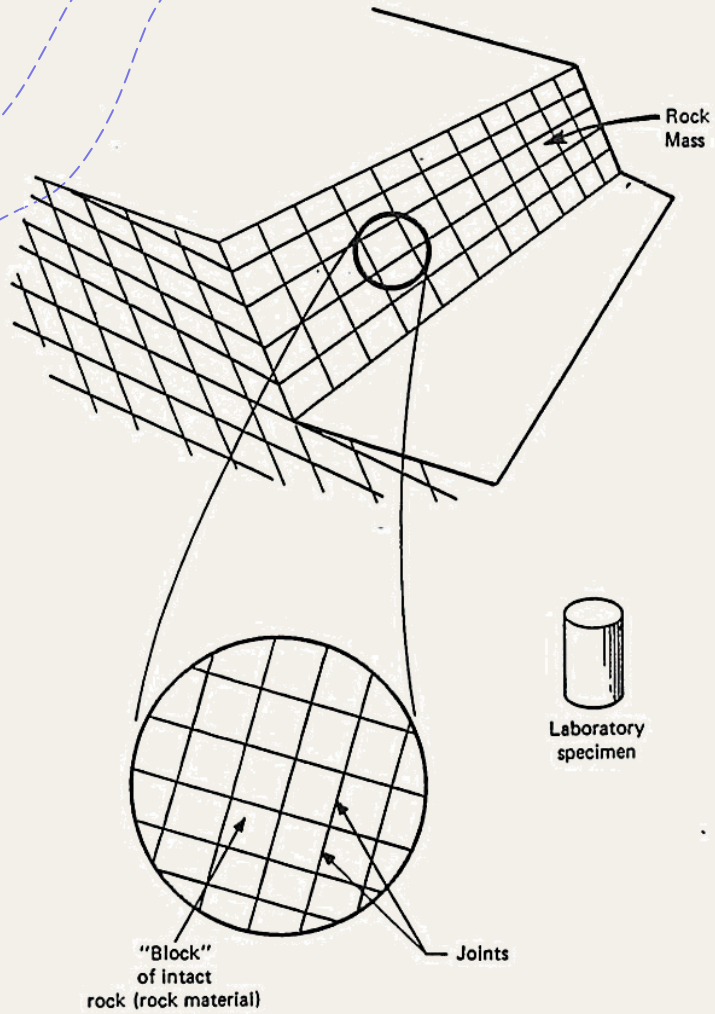
+ Ch3 岩石、岩體與工程(Part 3)
岩體的工程性質

授課教師：邱雅筑
2020/10/19

大綱

1. 岩體的概念
2. 岩石的強度、變形性及其相關特性
3. 岩石材料的力學性質
4. 不連續面(弱面)的力學性質
5. 岩體的力學性質

1. 岩體的概念



Definitions of rock mass and rock material.

岩體
(rock mass)
力學性質
(強度、變形性、
水力性質)
Mech. Properties
Strength, deformability,
hydraulics

=

+

完整岩石
(intact rock)

不連續面
(discontinuity)

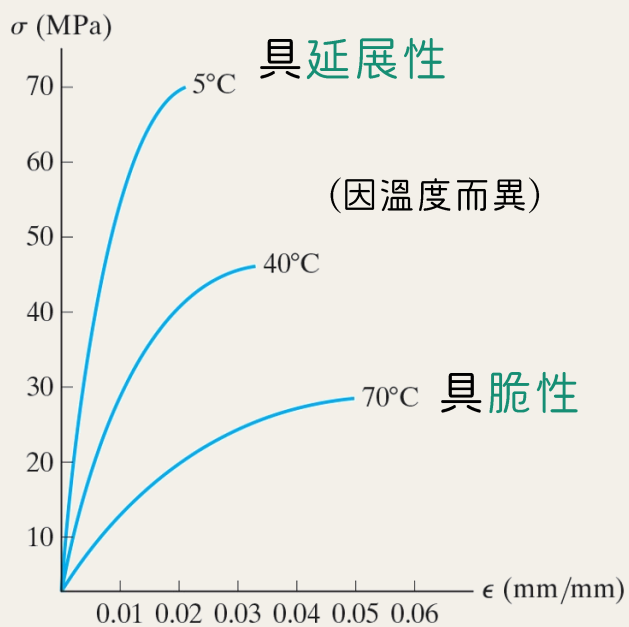
物質不連續
Discontinuity of the
material

力學性質不連續
Discontinuity in
Mechanics

2. 岩石的強度、變形性及其相關特性

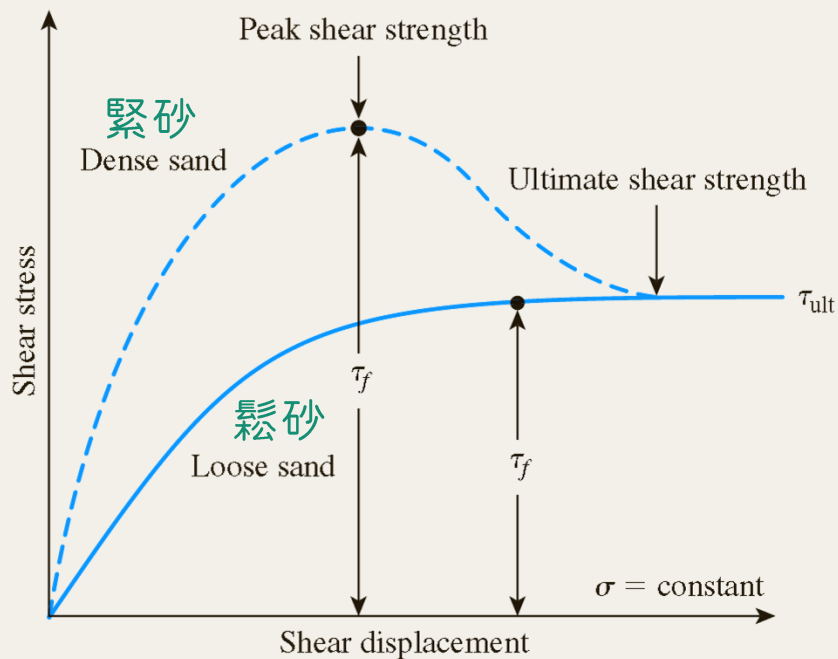
- + 室內試驗：直接剪力試驗、壓力試驗...
- + 應力 - 應變曲線
- + 延展性(ductile)材料：金屬
- + 脆性(brittle)材料：混凝土、土壤、岩石...

壓克力

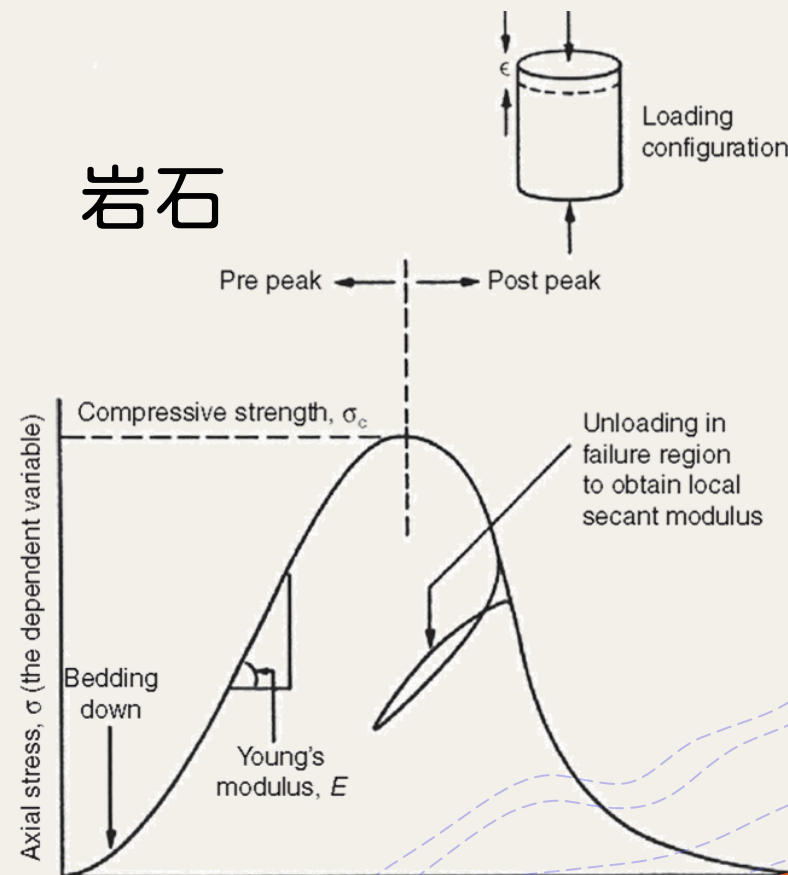


σ - ϵ diagrams for a methacrylate plastic

土壤



岩石



延展性材料

V.S.

脆性材料

金屬材料(受拉力破壞)



Necking



Failure of a
ductile material

混凝土(受壓力破壞)

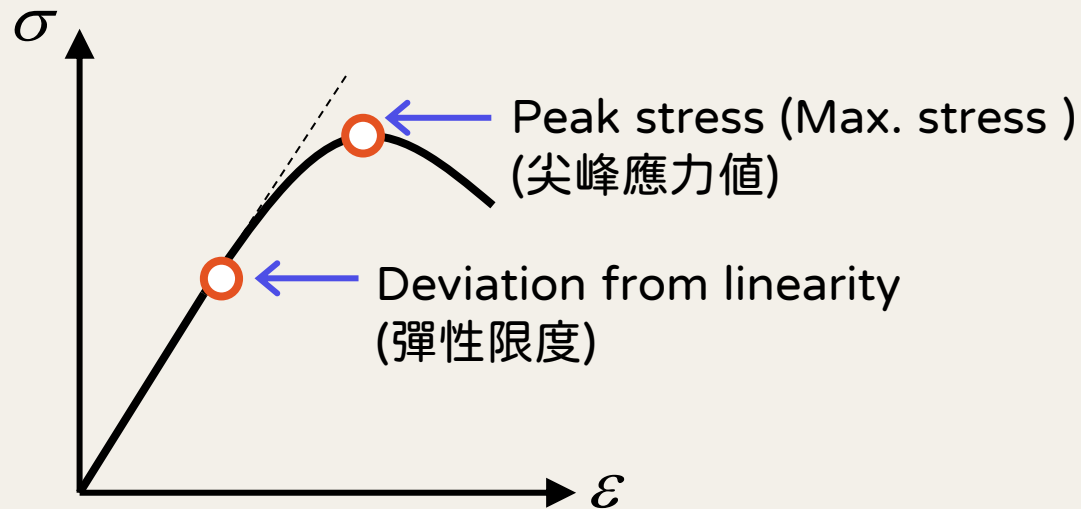


岩石的強度與變形性

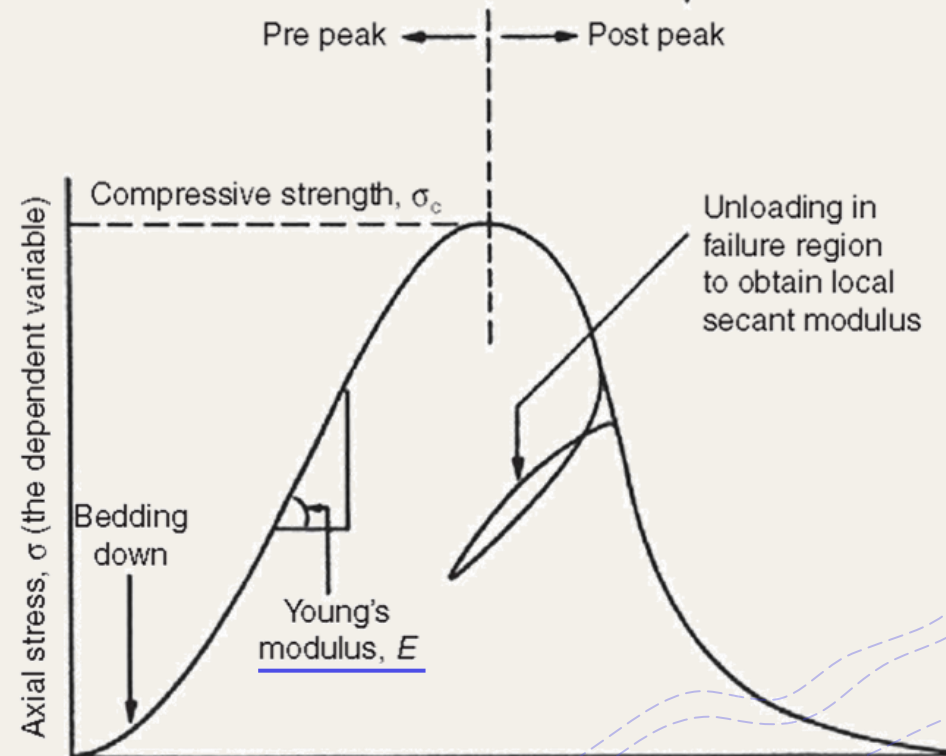
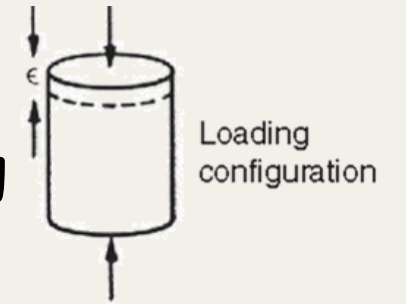
岩石的破壞：

尖峰應力發生位置，稱為岩石的強度

Failure \equiv peak stress (Max. stress)
(strength)



變形性：
達到強度前線性段的
斜率 (楊氏模數)



岩石的楊氏模數如何決定？

%強度的切線斜率
(通常用50%)

線性段部分的
平均斜率

%強度的割線斜率
(通常用50%)

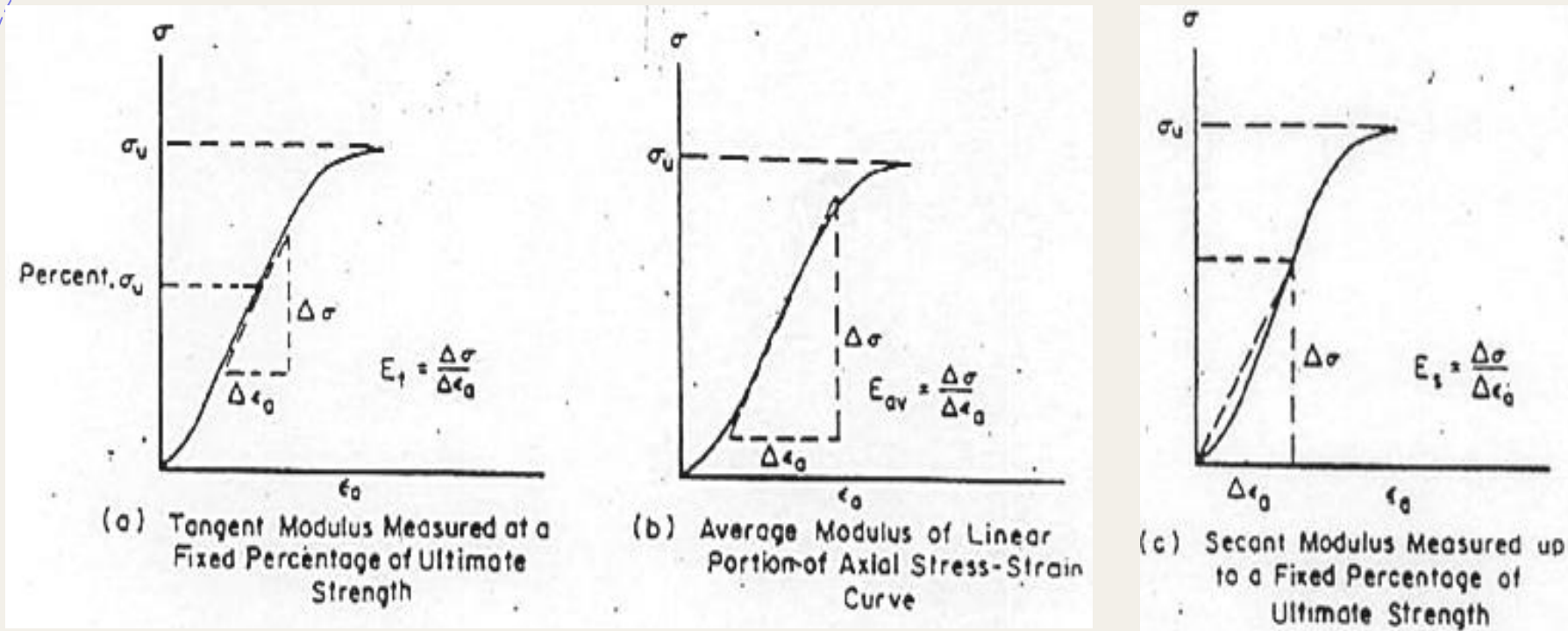


Fig. 2. Methods for calculating Young's modulus from axial stress-strain curve.

-Defined by ISRM(1981)

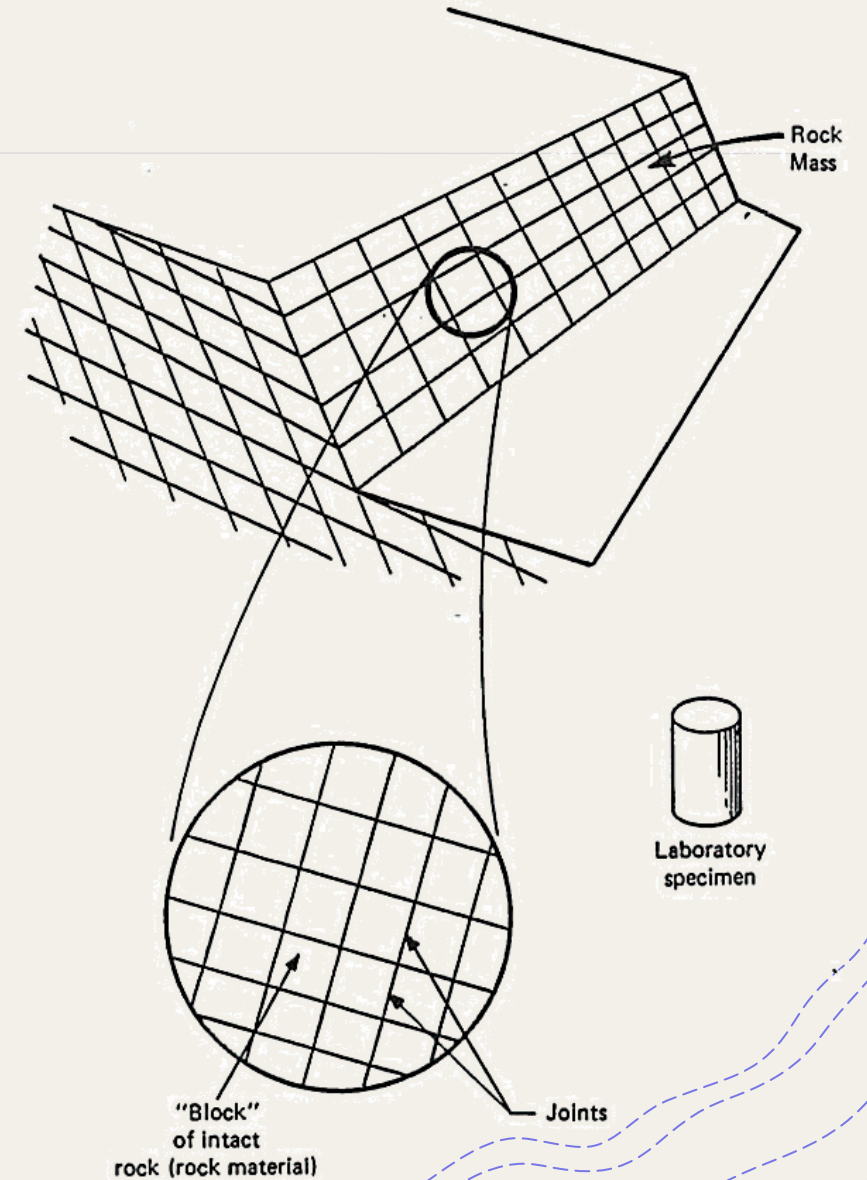
Scale effect (規模效應)

岩體(rock mass)



$$n = \frac{\text{joints spacing } (s)}{\text{range of influence } (c)}$$

	岩體	n
1	完整岩石材料 intact rock	10 ~ 1
2	部份岩石材料 intact rock ~ jointed rocks	1
3	A 開裂岩體 jointed rocks	1/10
	B 開裂岩體 Highly jointed rocks	1/100
4	高度破碎岩體 (土、堆石) gravels?	1/1000



Definitions of rock mass and rock material.

3. 岩石材料的力學性質

- + 指數特性：孔隙率、密度、透水性(滲透性)、強度、消散耐久指數、波速
- + 室內力學試驗：張力強度試驗、壓力強度試驗、剪力強度試驗
- + 岩石材料受壓的強度與變形性
- + 岩石材料的破壞準則：Mohr-Coulomb, Hoek-Brown
- + 現地試驗

圍壓由小→大

The image displays three cylindrical concrete specimens against a dark background. From left to right, the specimens show increasing levels of lateral pressure. The leftmost specimen is a smooth, intact cylinder. The middle specimen shows a distinct failure pattern with a vertical crack and a diagonal crack, indicating a transition from brittle to ductile behavior. The rightmost specimen is heavily crushed and fragmented, showing a complex failure pattern with multiple diagonal and vertical cracks, characteristic of a ductile failure under high lateral pressure. A green curved arrow points from left to right across the top of the specimens, with the text '圍壓由小→大' (Lateral pressure from small to large) written in green above it. The title '三軸壓力試驗' (Triaxial Pressure Test) is written in white in the center of the image.

三軸壓力試驗

增加圍壓可使岩石由脆性轉變為延展性

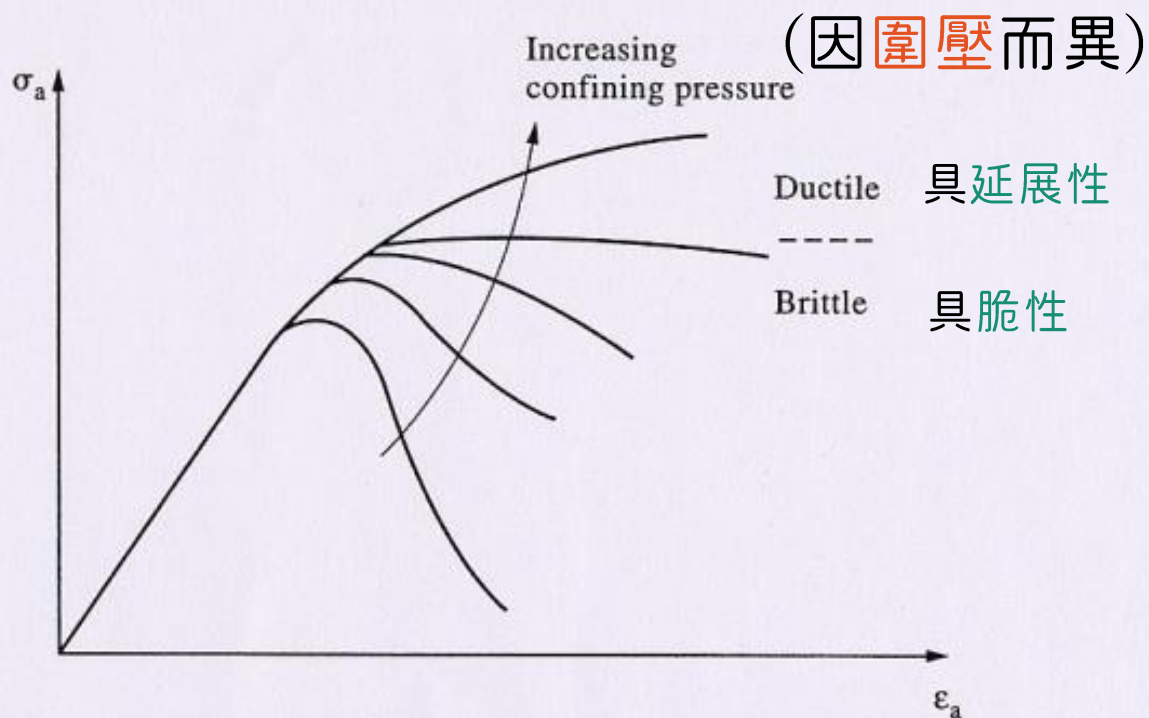
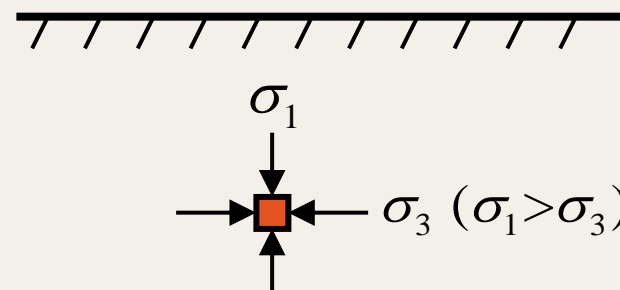


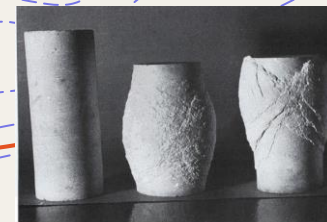
Figure 6.15 The effect of confining pressure in the triaxial test and the brittle-ductile transition.

圍壓？



圍壓 p 增加 

- (1) Brittle \rightarrow Ductile
- (2) Deformability \uparrow
- (3) Strength \uparrow
- (4) Failure pattern



Mohr - Coulomb Failure Criterion

(1) τ - σ plane

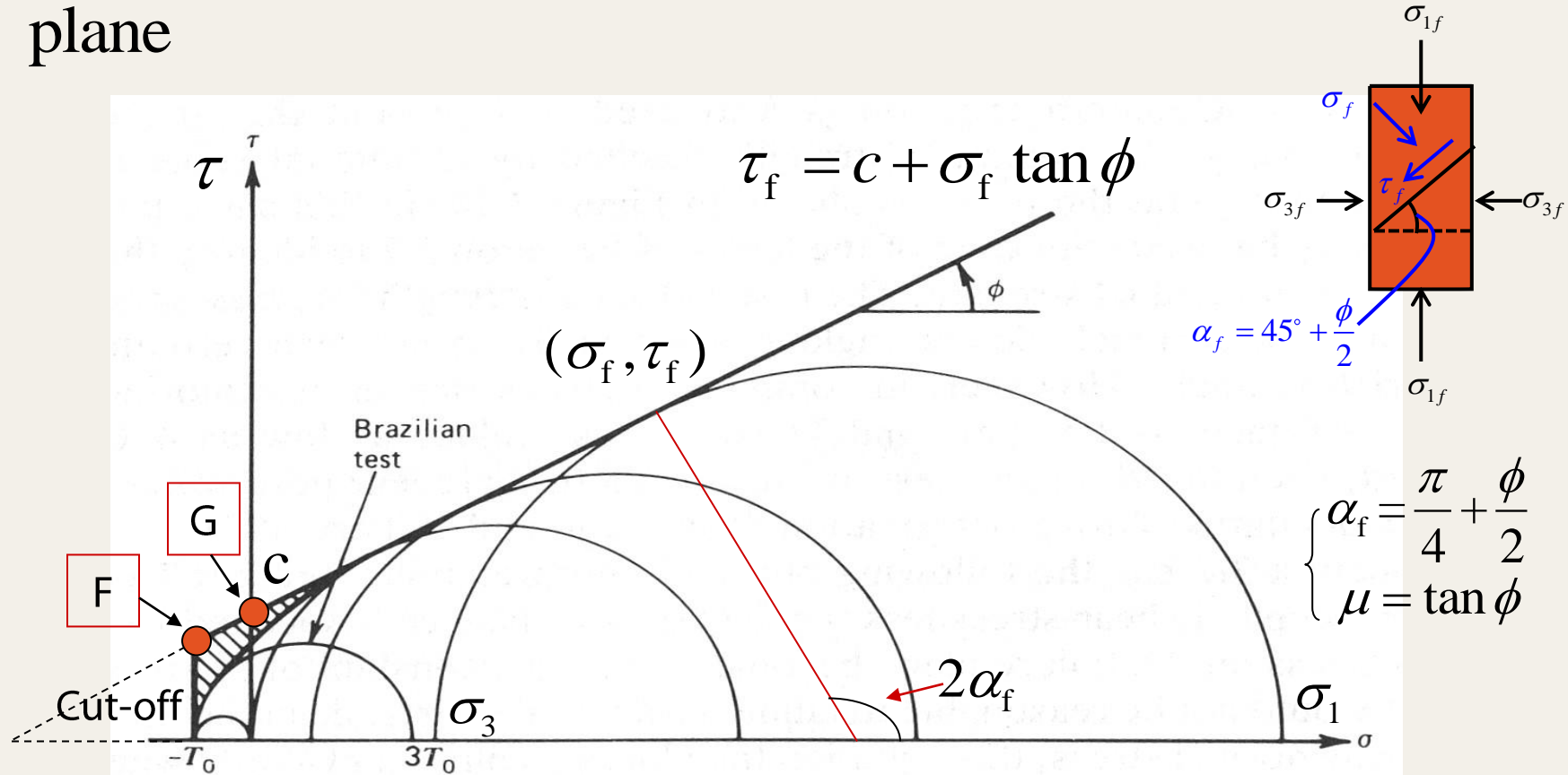
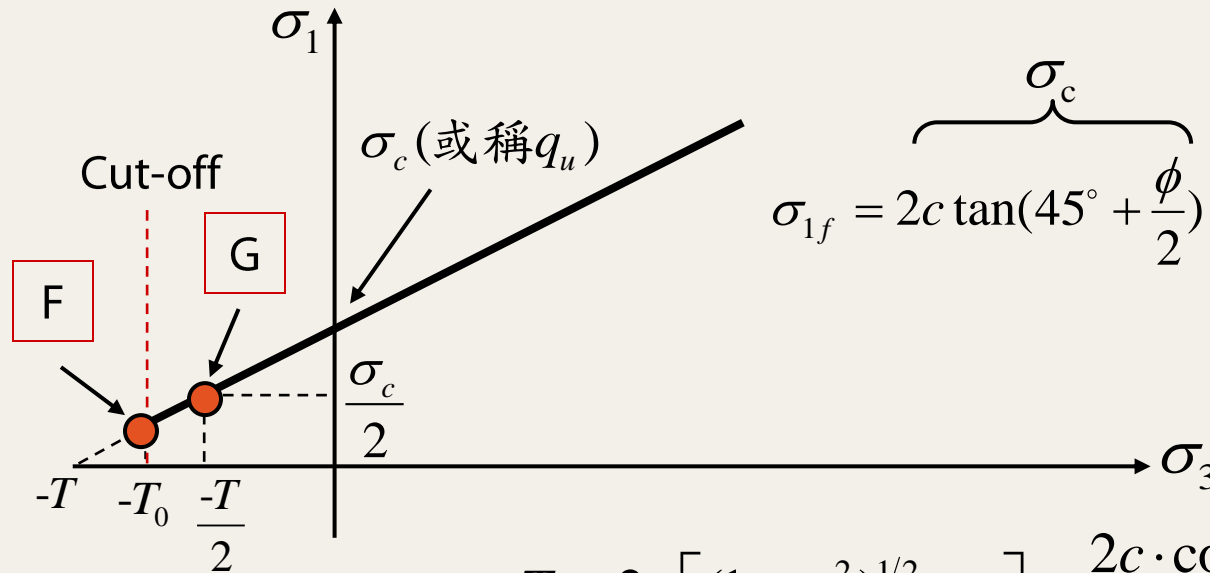


Figure 3.16 Comparison of empirical envelope and Mohr-Coulomb criterion in the tensile region. Inside the ruled region, the Mohr-Coulomb criterion with tension cutoff overestimates the strength.

Mohr - Coulomb Failure Criterion

(2) $\sigma_1 - \sigma_3$ plane



$$\sigma_{1f} = \underbrace{\sigma_c}_{2c \tan(45^\circ + \frac{\phi}{2})} + \sigma_{3f} \tan^2(45^\circ + \frac{\phi}{2})$$

T_0 : tensile strength

$$T = 2c \left[(1 + \mu^2)^{1/2} - \mu \right] = \frac{2c \cdot \cos \phi}{1 + \sin \phi} \quad (\text{apparent})$$

$$\sigma_c = 2c \left[(1 + \mu^2)^{1/2} + \mu \right] = \frac{2c \cdot \cos \phi}{1 - \sin \phi}$$

Hoek - Brown Failure Criterion(1980)

Hoek and Brown (1980a)

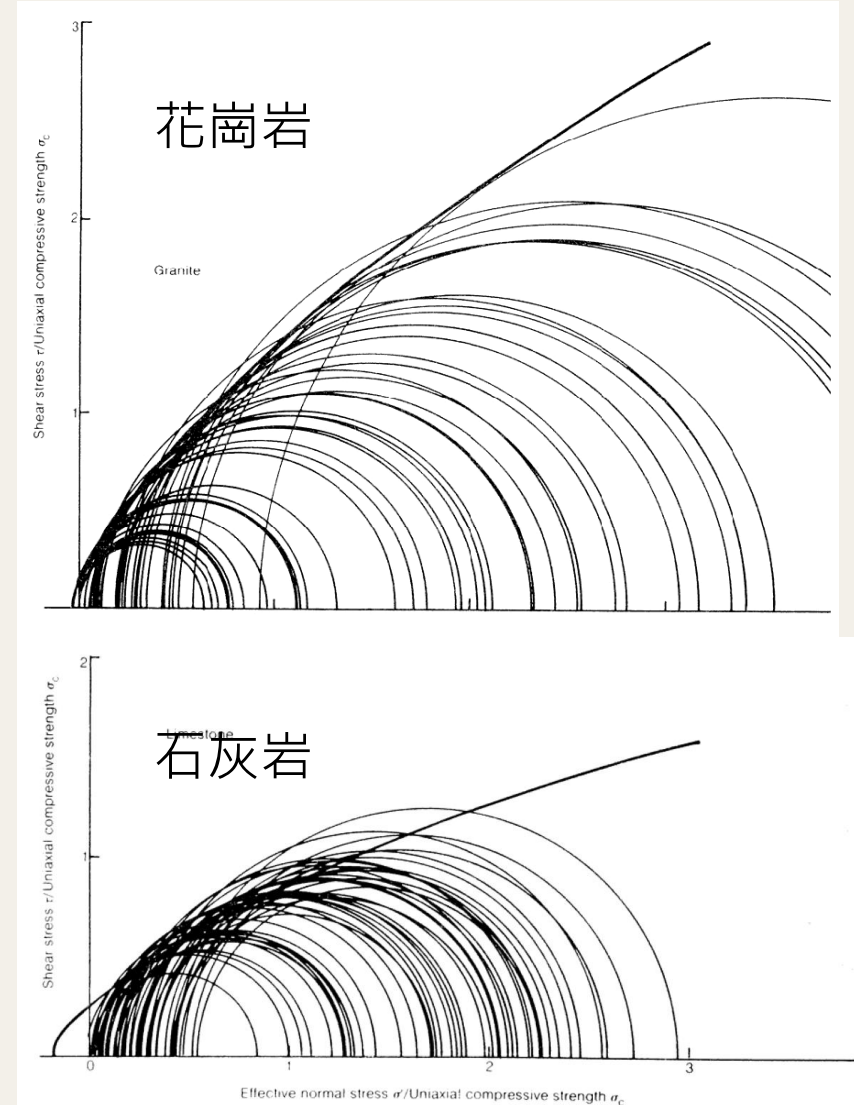
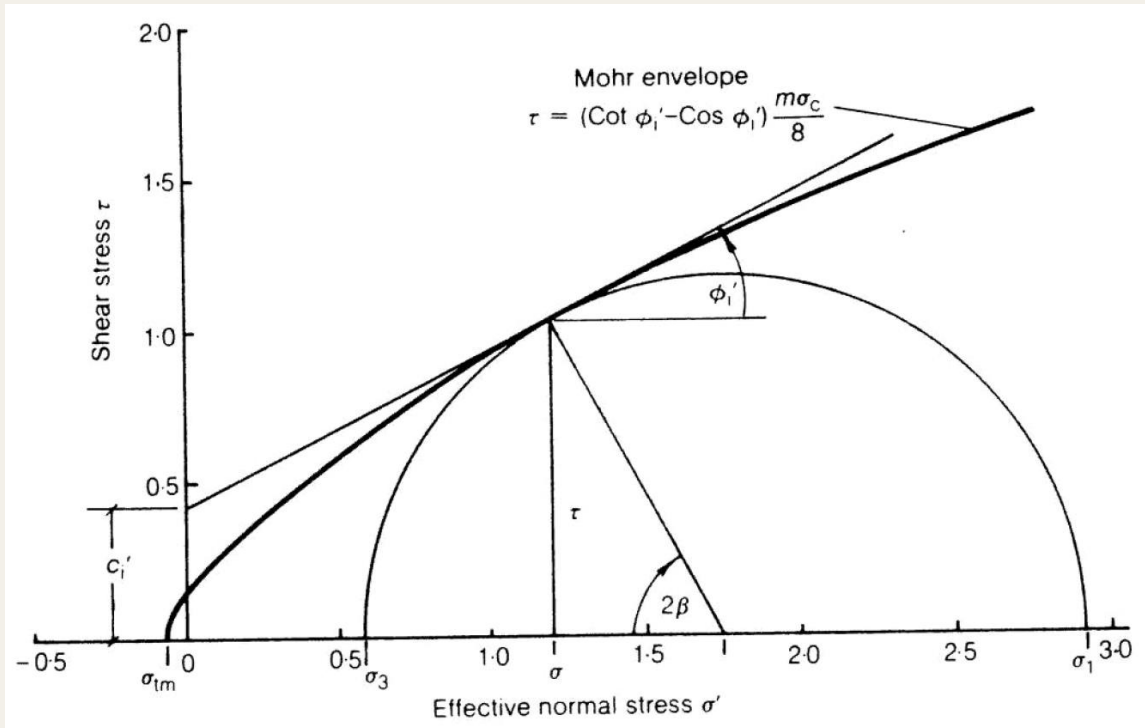
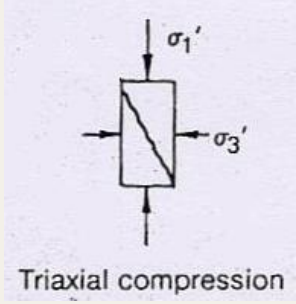
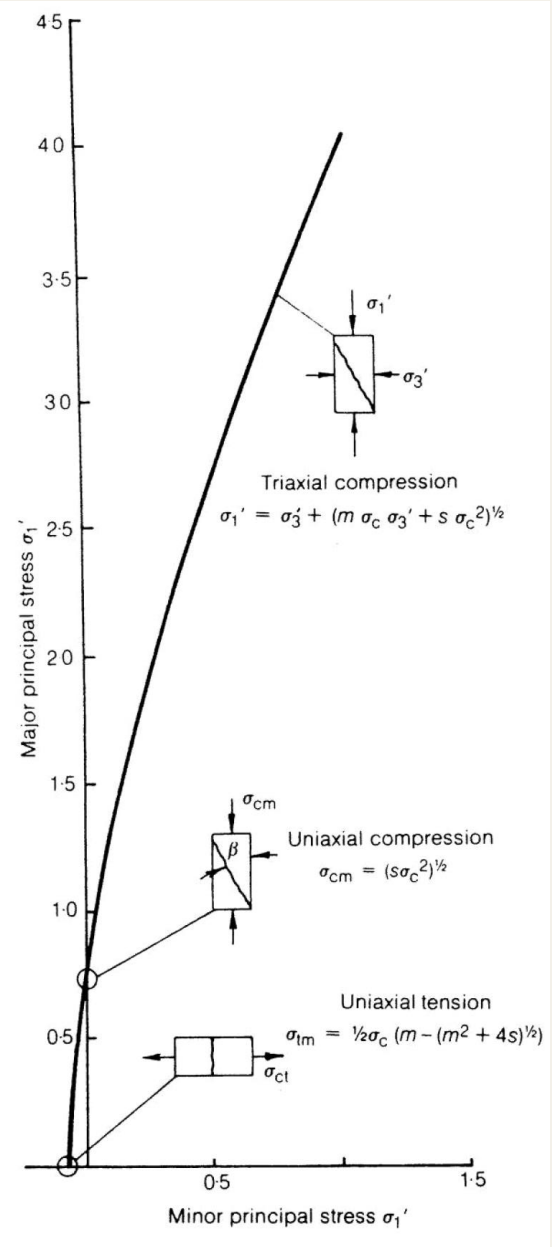


Figure 6 : Mohr failure circles for published triaxial test data for intact samples of (a) granite and (b) limestone.

Hoek - Brown Failure Criterion(1980)

(1) $\sigma_1 - \sigma_3$ plane



$$\sigma_1' = \sigma_3' + (m \sigma_c \sigma_3' + s \sigma_c^2)^{1/2}$$

m: 完整岩材內顆粒大小 (ϕ 有關)

s: 岩體破碎程度 (c有關)

Figure 3. Summary of equations with the non-linear failure criterion proposed by Hoek & Brown (1980b)

4.不連續面的力學性質

1. 不連續面的描述與評估：位態、間距、持續性、粗糙度、內壁材料強度、內寬、軟弱夾心、滲水情形、組數、弱面密度與岩體幾何形狀
2. 不連續面的室內力學試驗：剪力強度試驗(正向、剪向)
3. 不連續面的強度與變形性
4. 不連續面的破壞準則：Mohr-Coulomb, Barton

4.1 不連續面的描述與評估

參考第二章

- + 位置、方位
- + 間距
- + 持續性
- + 粗糙度
- + 內壁材料強度
- + 內寬
- + 軟弱夾心
- + 滲水情形
- + 組數
- + 弱面密度與岩體幾何形狀

4.2 不連續面的室內力學試驗

Li et al. (2016) 岩石節理試體照片

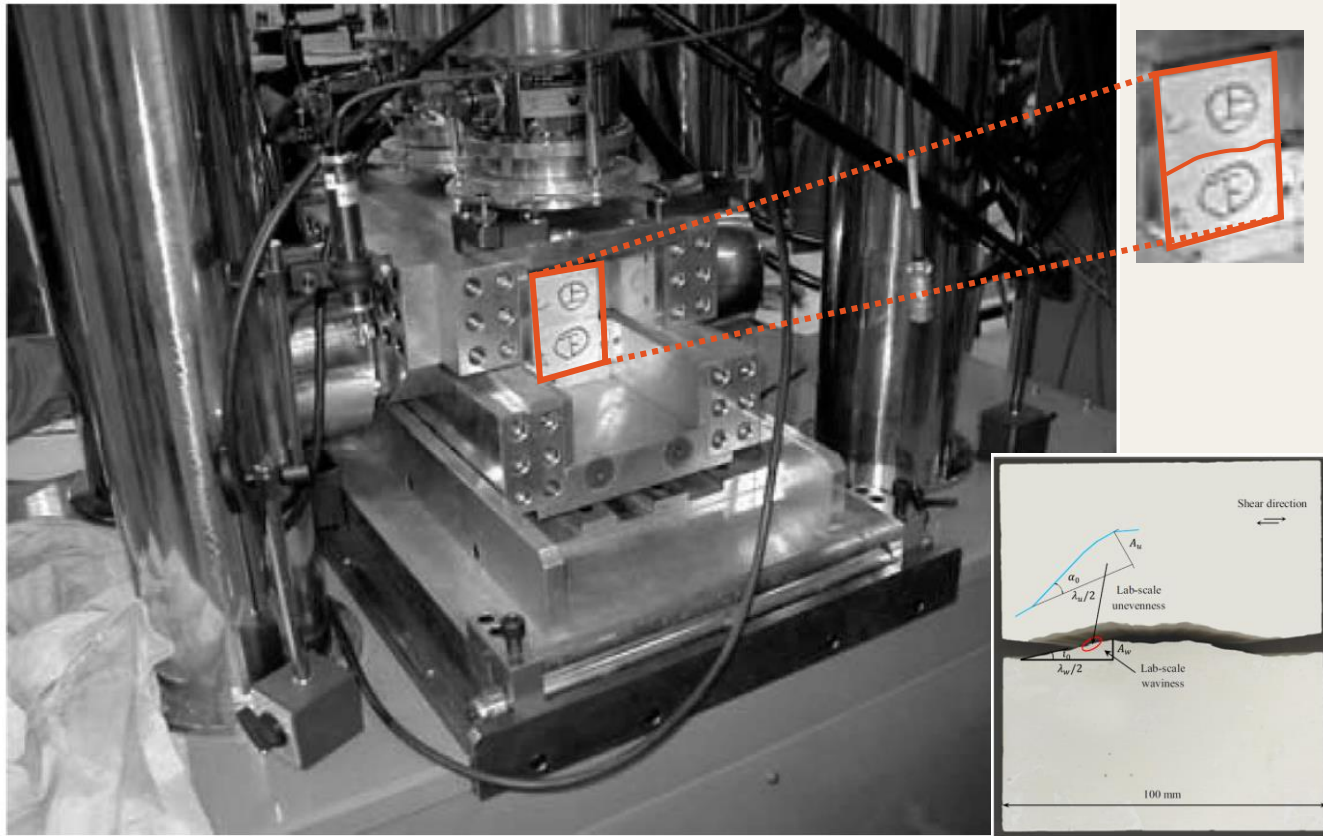


Photo 2 Shear test box.

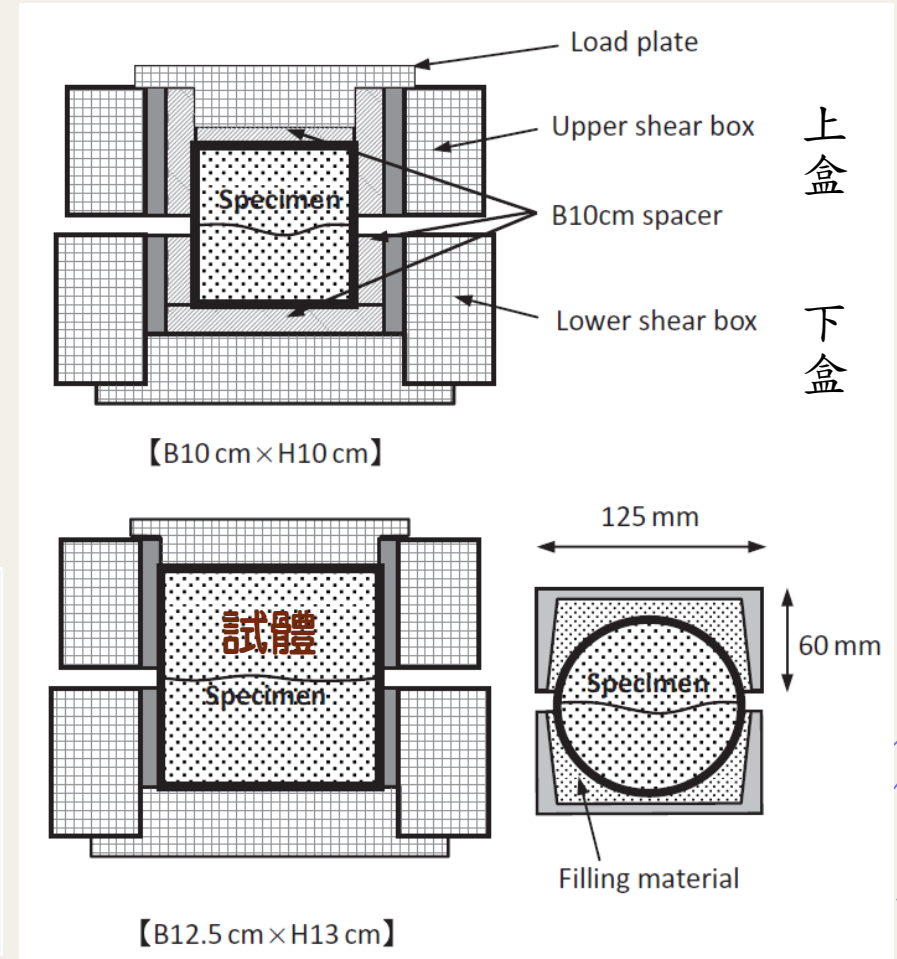


Figure 3 Structure of shear box and preparation of artificial joint sample.

Jiang, Y. J. (2016). Rock joints shearing testing system in X.T . Feng (Ed.), *Rock Mechanics and Engineering* Vol. 2 (pp. 217-249). London, UK: Taylor & Francis Group.

4.3 不連續面的強度與變形性

+ 正向應力 & 正向位移

+ 閉合曲線

+ σ & Δv 關係

+ 剪應力 & 剪位移

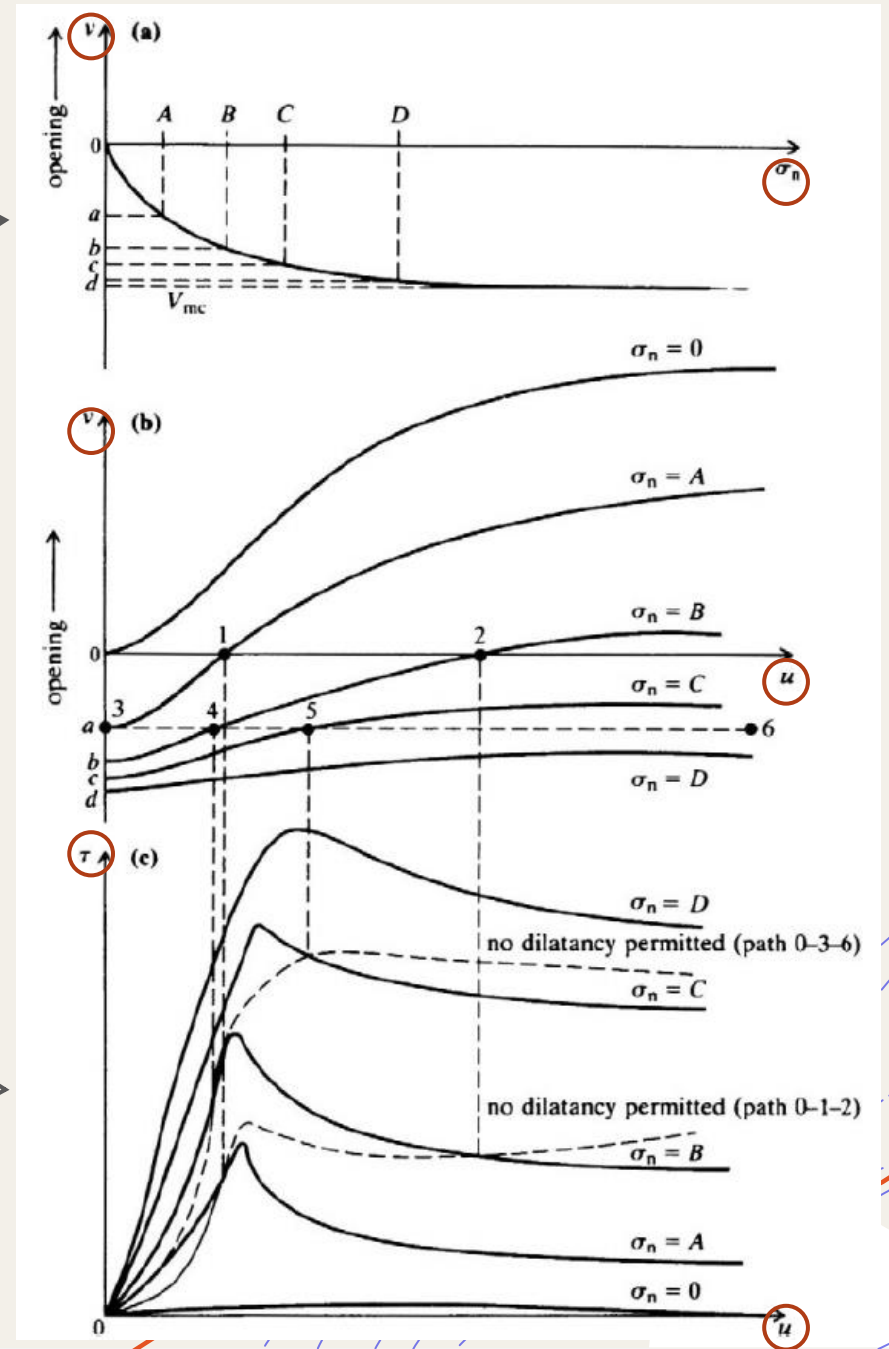
+ 剪力變形曲線

+ τ & Δu 關係

+ 剪位移 & 正向位移

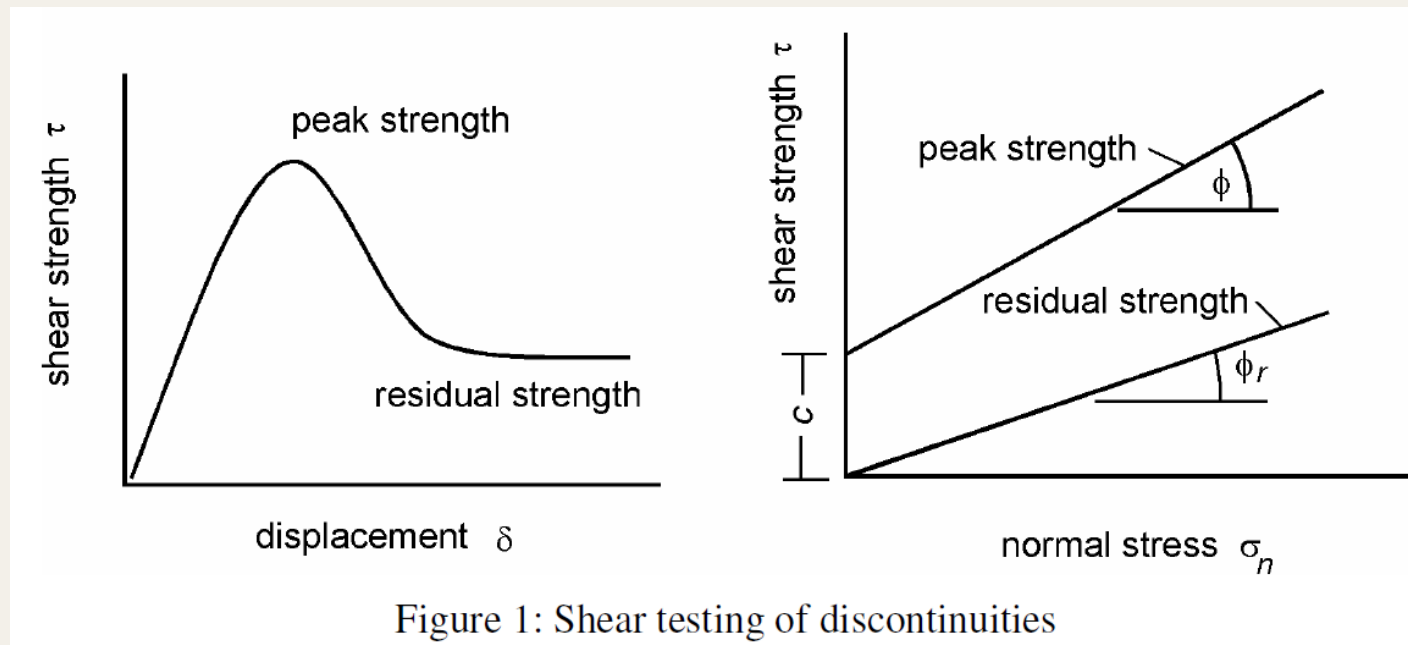
+ 膨脹曲線(剪動時垂直向位移的變化)

+ Δu & Δv 關係



不連續面的剪力強度

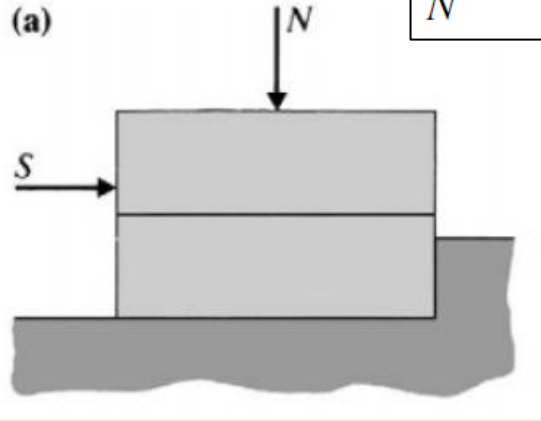
1. 尖峰摩擦角, ϕ_p
2. 殘餘摩擦角, ϕ_r
3. 基本摩擦角, ϕ_b (basic friction angle)



表面粗糙度對剪力強度的影響

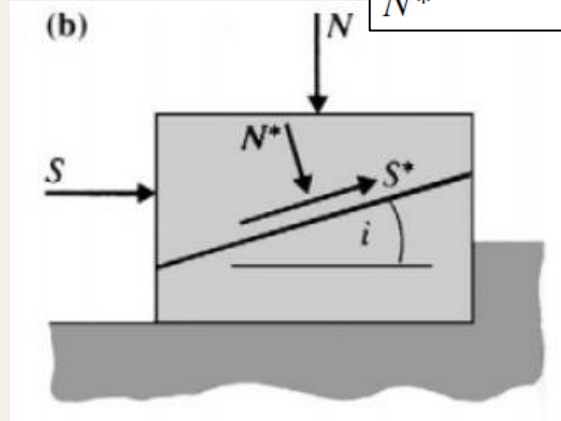
平滑弱面

$$\frac{S}{N} = \tan \phi$$



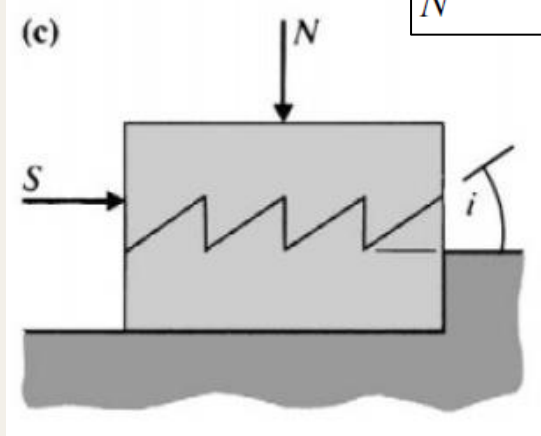
平滑弱面+傾斜

$$\frac{S^*}{N^*} = \tan \phi$$



規則起伏(鋸齒狀)弱面

$$\frac{S}{N} = \tan (\phi + i)$$



$$\frac{S}{N} = \tan (\phi + i)$$

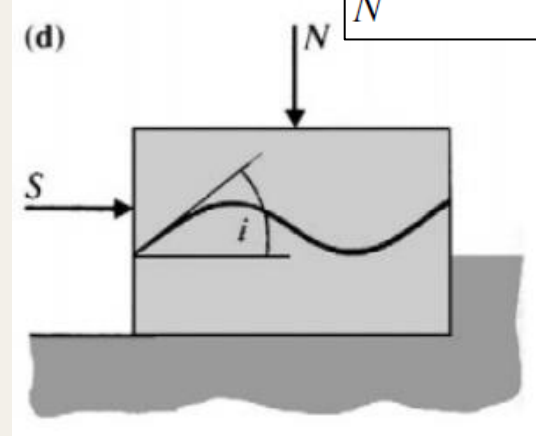
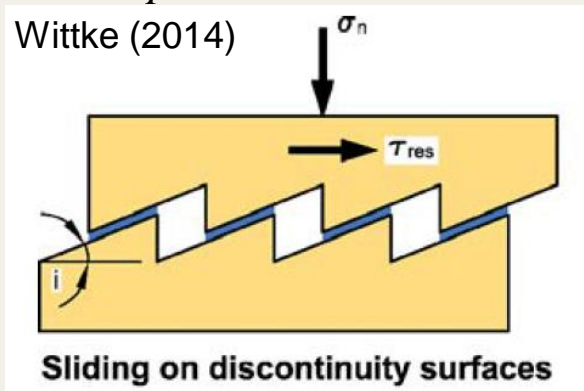


Figure 4.41 Idealised surface roughness models illustrating the roughness angle, i .

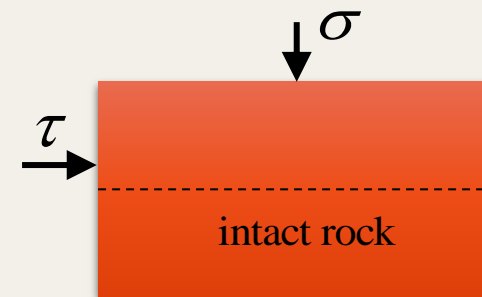
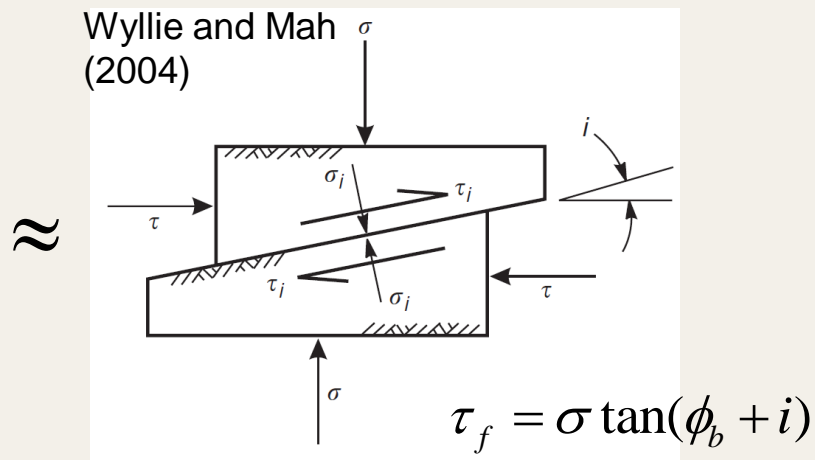
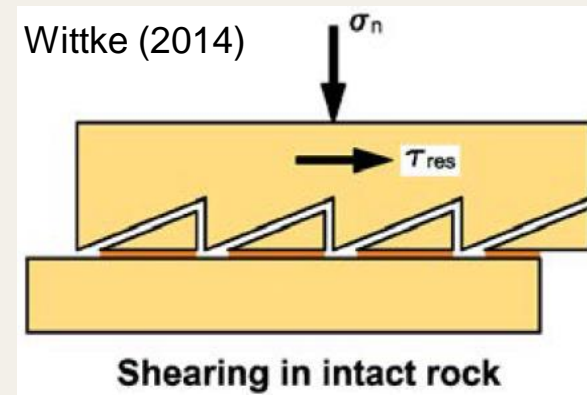
Brady and Brown (2005)

不連續面之力學行為:(1)爬坡 ; (2)剪斷

+ (1) $\frac{\sigma}{\sigma_T} \ll 1$ 爬坡 (sliding up)



+ (2) $\frac{\sigma}{\sigma_T} \approx 1$ 剪斷 (shearing)



$\tau_f = c_0 + \sigma \tan \phi_0$ $c_0 > \phi_0$: intact rock

4.4 不連續面的破壞準則

+Patton's Bilinear model (1966)

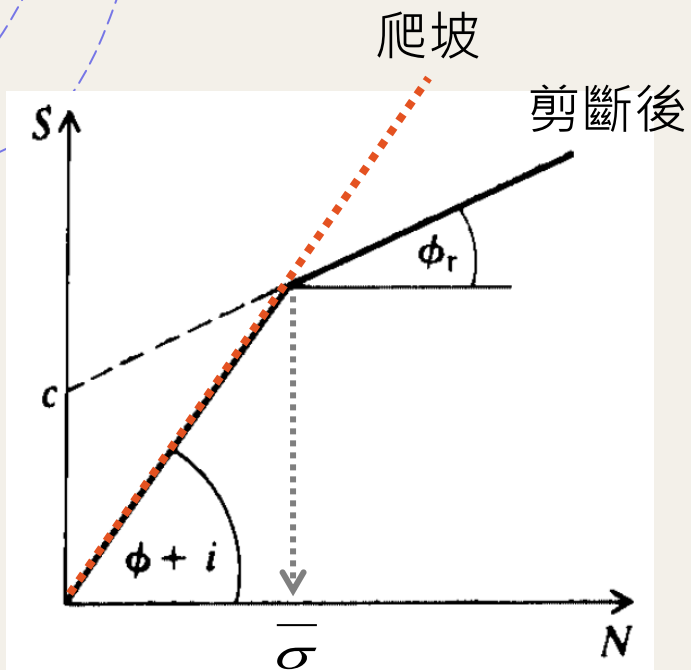
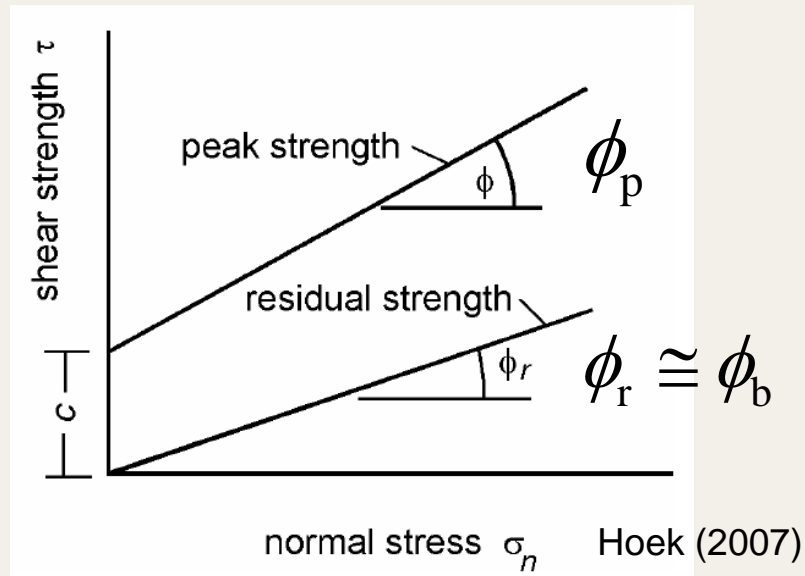


Figure 4.42 Bilinear peak strength envelope obtained in direct shear tests on the models shown in Figure 4.41.

Brady and Brown (2005)



$\bar{\sigma}$: 轉換應力

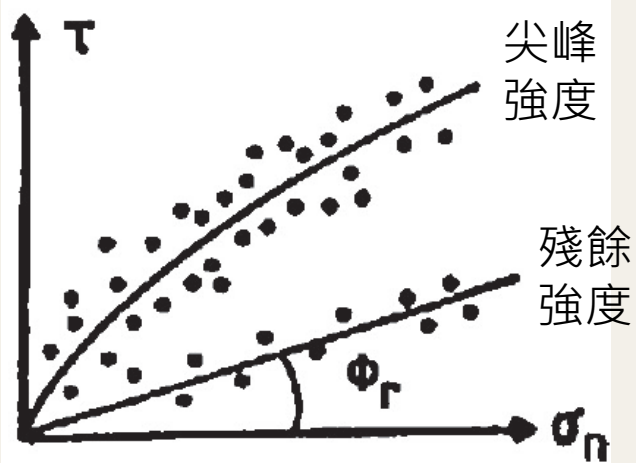
$\sigma < \bar{\sigma}$: joint 爬坡 $\rightarrow \phi_p$

$\sigma > \bar{\sigma}$: intact rock 破壞 $\rightarrow \phi_r \cong \phi_b$

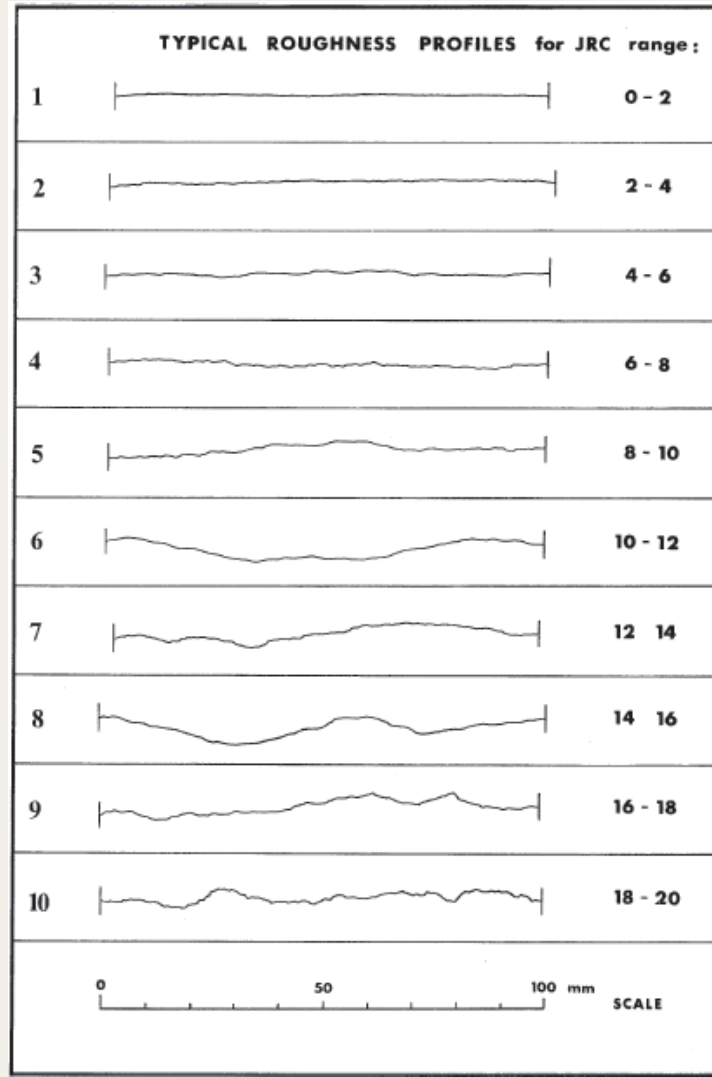
4.4 不連續面的破壞準則

$$\tau = \sigma_n \tan \left[\overset{\text{參數}}{\text{JRC}} \log \left(\frac{\text{JCS}}{\sigma_n} \right) + \Phi_r \right]$$

節理粗糙(度)係數
JRC = joint roughness coefficient
 單軸壓縮強度
JCS = joint wall compression strength
 Φ_r = residual friction angle



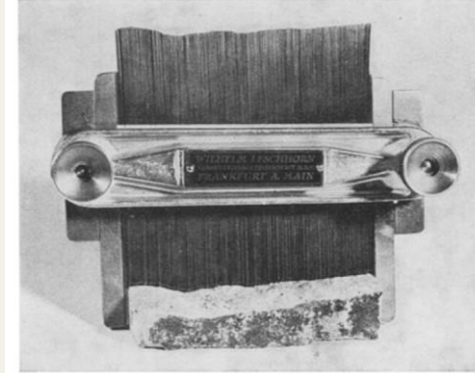
Barton (2013)



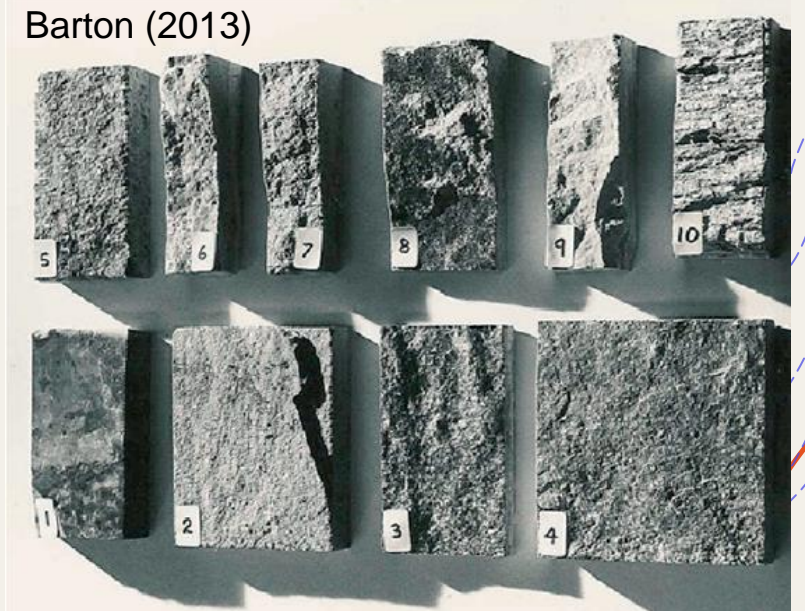
Barton and Choubey (1977)

B-B model

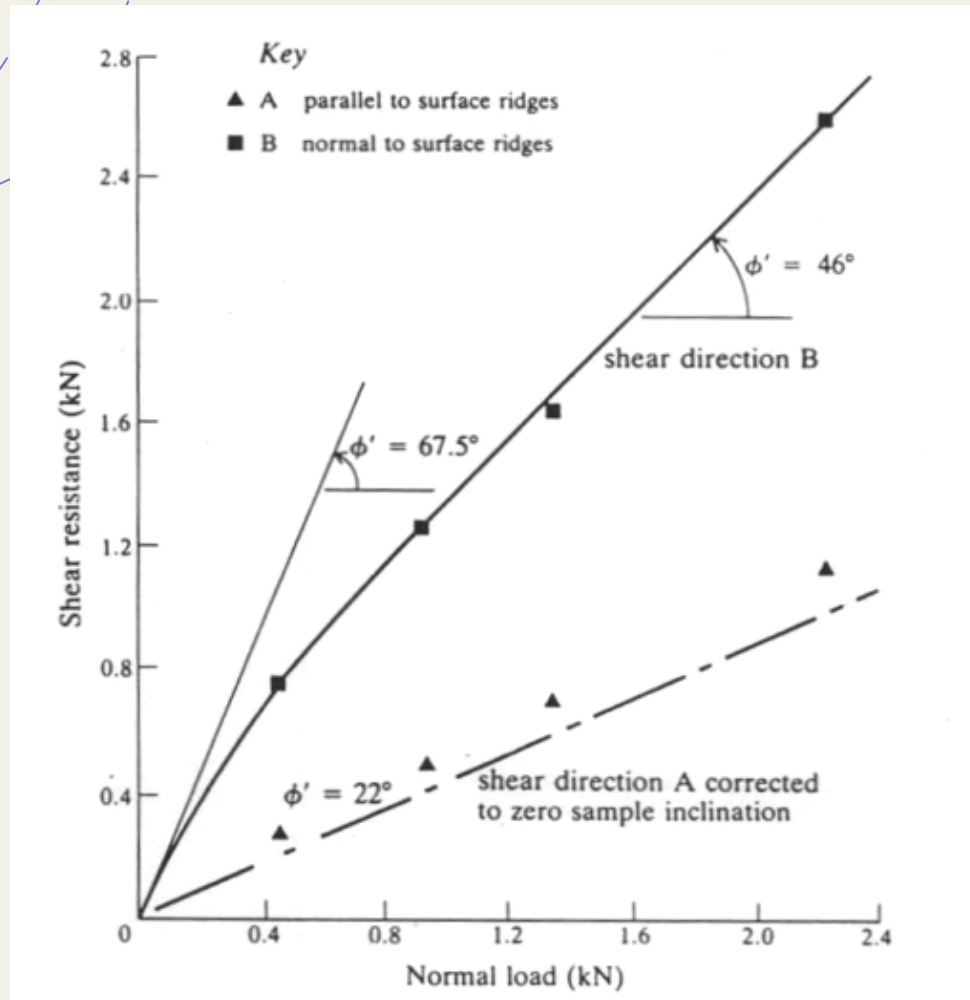
Barton and Choubey (1977)



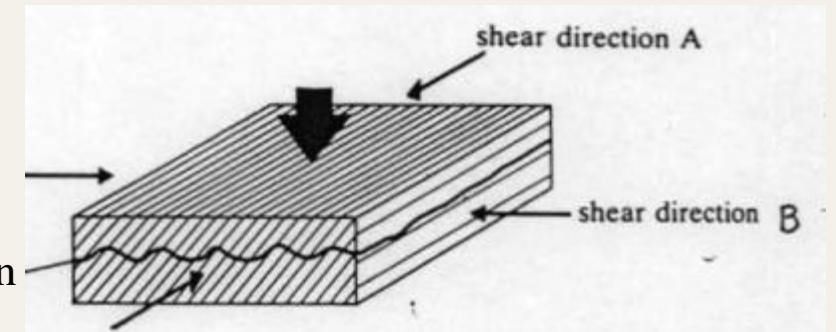
Barton (2013)



不連續面強度之異向性



intersection lineation



Effect of shearing direction

不連續面強度之異向性

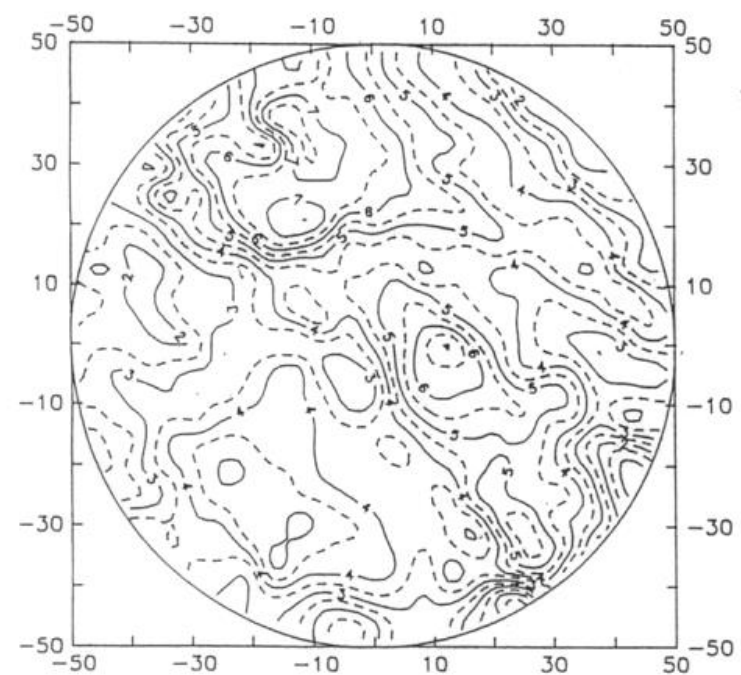
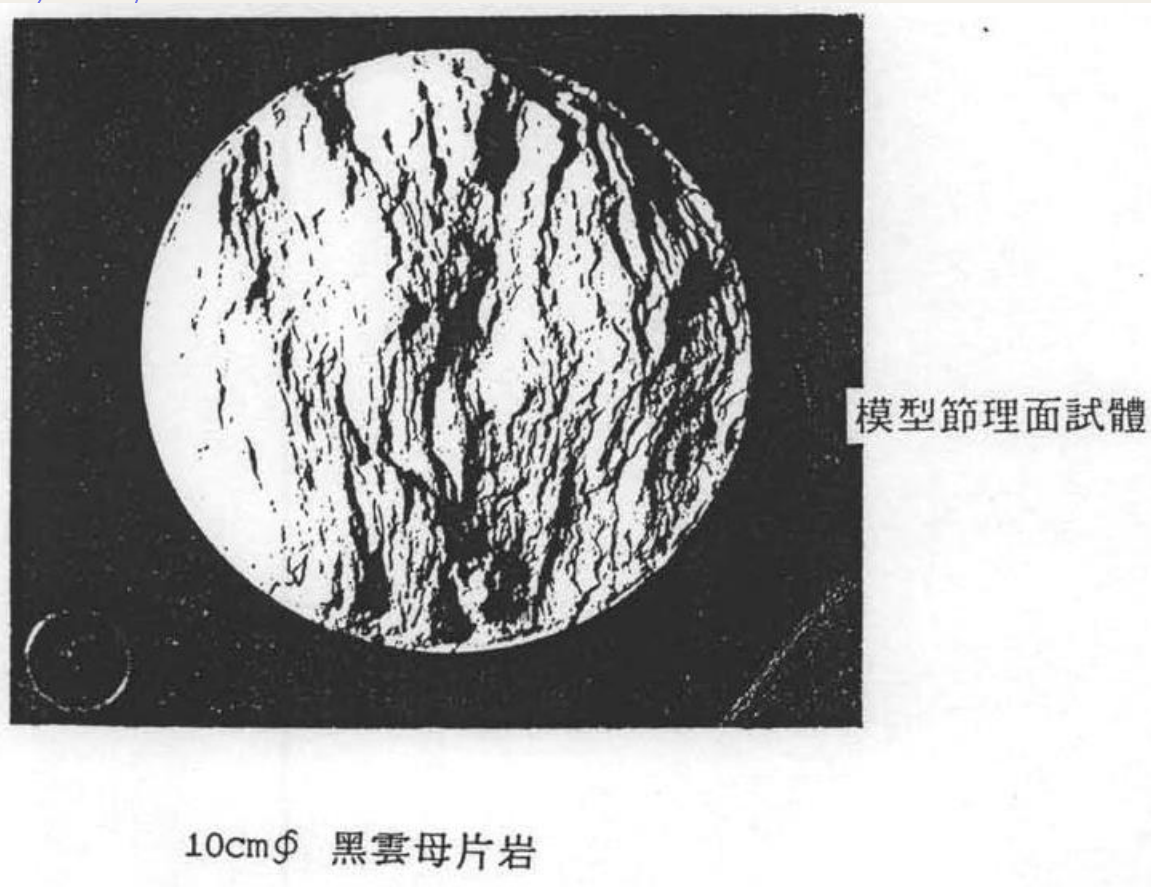
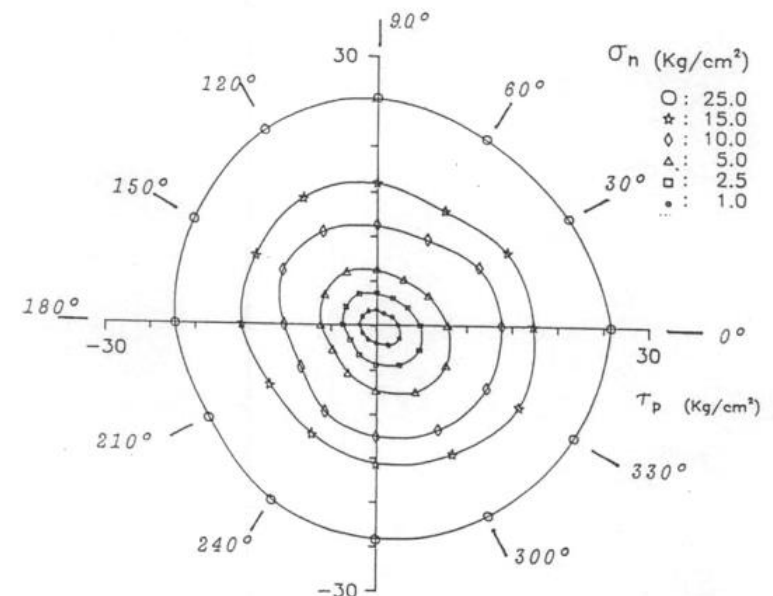


圖3.11 節理面等高線圖 (a)正方形試體, (b)圓形試體 (單位:mm)

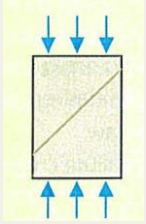


岩石節理面異向性(剪力強度)

5. 岩體的力學性質

1. 數學模式：Jaeger's single plane of weakness theory, Bray's superposition theory...
2. 室內實驗
3. 現地實驗
4. 數值模擬
5. 經驗統計法：**岩體分類法**

5.1 岩體之強度(數學模式)



+ 含單一節理(裂面)之岩體強度

- a) intact rock fracture mode
- b) joint sliding mode
- c) Jaeger's single plane of weakness theory (1960)

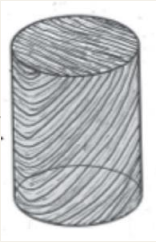
Vallejo and Ferrer (2011)



+ 含多條裂面之岩體強度

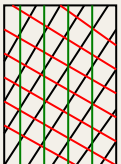
- a) Bray's superposition principle

Hencher (2015)



+ 含一組節理之岩體強度

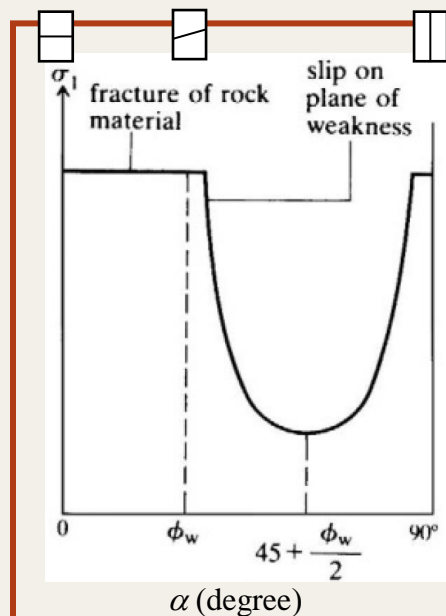
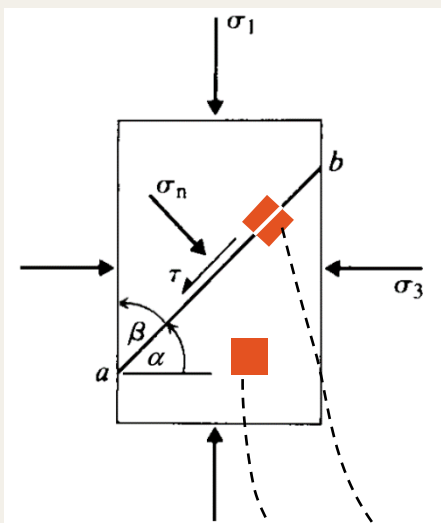
- a) Intact rock fracture mode
- b) Joint sliding mode
- c) Mixed mode



+ 含多組節理之岩體強度

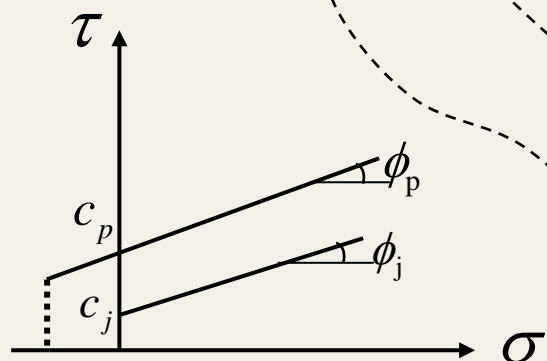
- a) 趨向isotropic → Hoek-Brown failure criterion

含單一裂面(弱面)之岩體強度



兩種破壞型態：

- 岩石材料破壞
 - 任一處剪應力 $> \tau_f$
- 沿著弱面滑動
 - 弱面上的剪應力 $> \tau_j$



- 岩石材料之破裂 (c_p , ϕ_p)

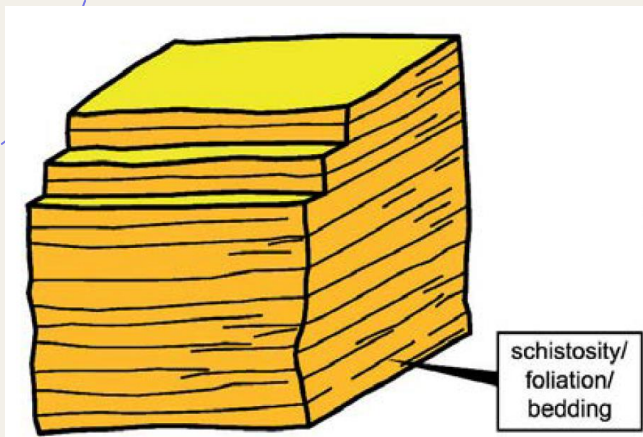
$$\tau_f = c_p + \sigma \tan \phi_p$$

- 岩石弱面之滑動 (c_j , ϕ_j)

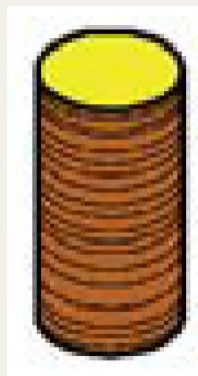
$$\tau_j = c_j + \sigma \tan \phi_j$$

含一組節理之岩體強度

現場岩體

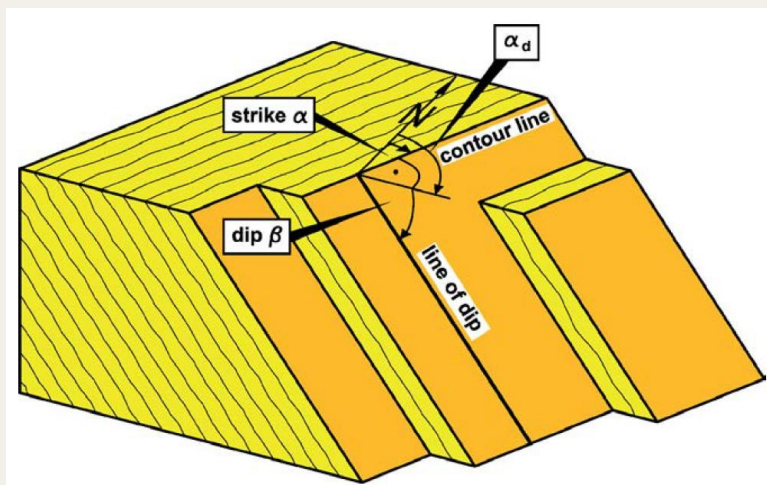
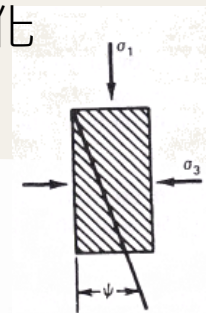


室內實驗



Wittke (2014)

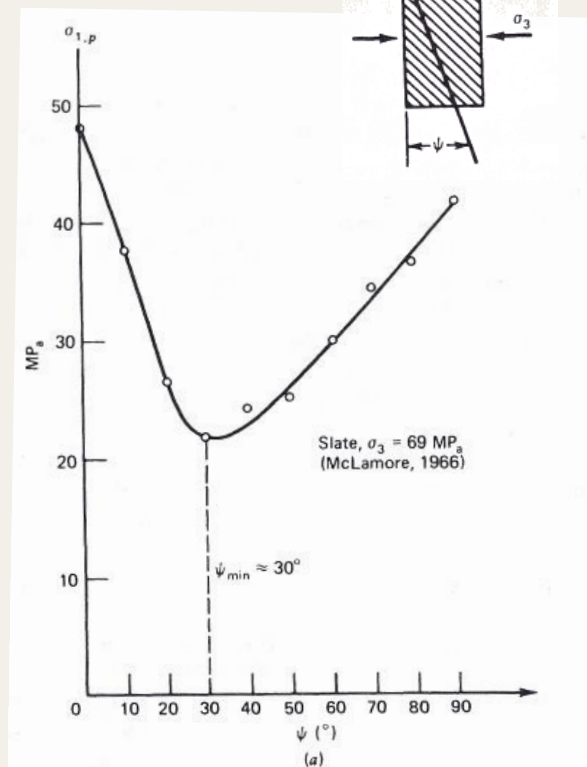
含一組節理岩體的強度隨不同 ψ 之變化



Wittke (2014)

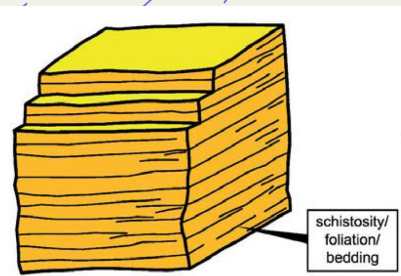


Hencher (2015)

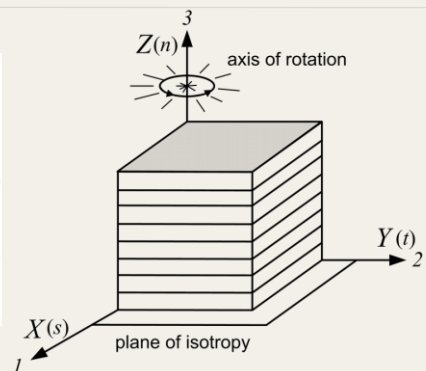


Goodman (1989)

岩體變形性

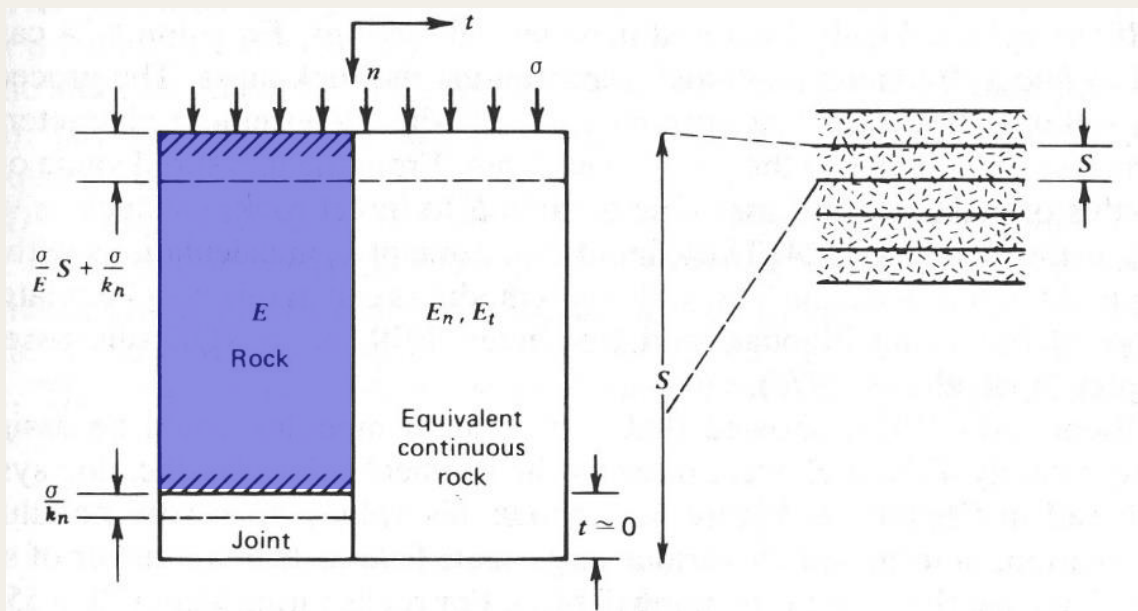


Wittke (2014)



橫向等向性材料
5個材料參數

$$E_n, G_{ns}, \nu_{sn}, E_s, \nu_{st}$$



+ 岩體楊氏模數經驗公式之統整

Table 3.25 EMPIRICAL EXPRESSIONS FOR ESTIMATING THE DEFORMATION MODULUS IN ISOTROPIC ROCK MASSES

Criterion	Application
$E = 2 \text{ RMR} - 100$ (GPa) (Bieniawski, 1978)	<ul style="list-style-type: none"> Good quality rock masses, $\text{RMR} > 50-55$ Not valid for low quality rock masses
$E = 10^{(\text{RMR}-10)/40}$ (GPa) (Serafim & Pereira, 1983)	<ul style="list-style-type: none"> Fair-low quality rock masses, $10 < \text{RMR} < 50$ Especially indicated for values $1 < E < 10$ GPa Too high values are obtained for low-very low quality rock masses
$E = \left(1 - \frac{D}{2}\right) \sqrt{\frac{\sigma_{ci}}{100}} 10^{(\text{GSI}-10)/40}$ (σ_{ci} in MPa; E in GPa) (Hoek et al., 2002)	<ul style="list-style-type: none"> Indicated for weak or soft rock masses with low or very low quality ($\text{GSI} < 25$) and intact rock with $\sigma_{ci} < 100$ MPa D (disturbance factor) = 0 (undisturbed rock mass) to 1 (fully disturbed)
$E = 100,000 \left(\frac{1-D/2}{1+e^{(75+25D-\text{GSI})/11}} \right)$ (E in MPa) (Hoek & Diederichs, 2006)	<ul style="list-style-type: none"> Valid for $\text{GSI} = 20$ to 80 $D = 0$ (undisturbed rock mass) $D = 1$ (fully disturbed)
$E = 10Q_c^{1/3}$ (E in GPa) (Barton, 1995, 2006)	<ul style="list-style-type: none"> Indicated for jointed or fractured rock masses
$E = 10^{(\nu_p - 0.5)/3}$ (ν_p in km/s; E in GPa) (Barton, 2006)	<ul style="list-style-type: none"> Rock mass properties are considered (ν_p picks up density and strength)

E = Rock mass empirical static deformation modulus.
 E_i = Intact rock deformation modulus measured in laboratory.
 RMR = Rock Mass Rating.
 GSI = Geological strength index.
 Q = Quality index.
 $Q_c = Q \cdot \sigma_{ci} / 100$ (σ_{ci} in MPa).
 σ_{ci} = Intact rock uniaxial compressive strength.
 ν_p = P wave velocity.

- These correlations have not yet been sufficiently verified.
- They give approximate, merely indicative values.
- In general, they overestimate the value of the rock mass deformation modulus.
- They do not take the possible anisotropic nature of the *in situ* deformation modulus into account.
- For the rock mass, a range of values is recommended between 0.4E and 1.6E.

岩體變形與強度之量測與試驗

一. 靜態方法

1) 室內試驗

+ Uniaxial compressive test, Triaxial compressive test

2) 現地試驗

a) **Plate bearing test (平鈹載重試驗)**

b) Pressure tunnel test

+ Hydraulic pressure chamber test

+ **Radial jacking test**

c) Borehole test

+ **Borehole dilatometer**

+ Borehole jack: Goodman's jack

d) Flat jack test

e) **Back analysis**

二. 動態方法

1) 室內試驗

a) Resonance method

+ Longitudinal vibration

+ Flexural vibration

+ Torsional vibration

b) Ultrasonic pulse method

2) 現地試驗

5.2 岩體室內試驗

+ 楊氏模數、單壓強度、巴西人張力強度之異向性



Fig. 9. Comparison of post failure specimens obtained from Boryeong shale laboratory tests (from [2], top) and bonded-particle DEM modeling (bottom). After (a) uniaxial compressive strength tests and (b) Brazilian tensile strength tests. (For interpretation of references to color in this figure, the reader is referred to the web version of this article.)

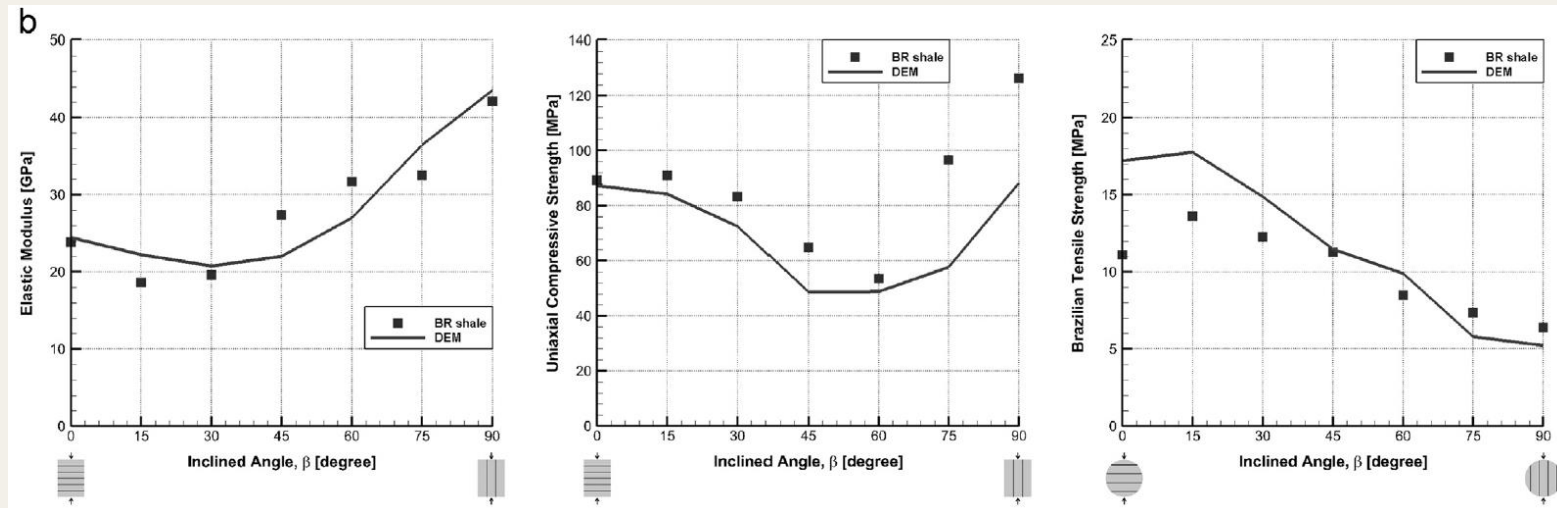
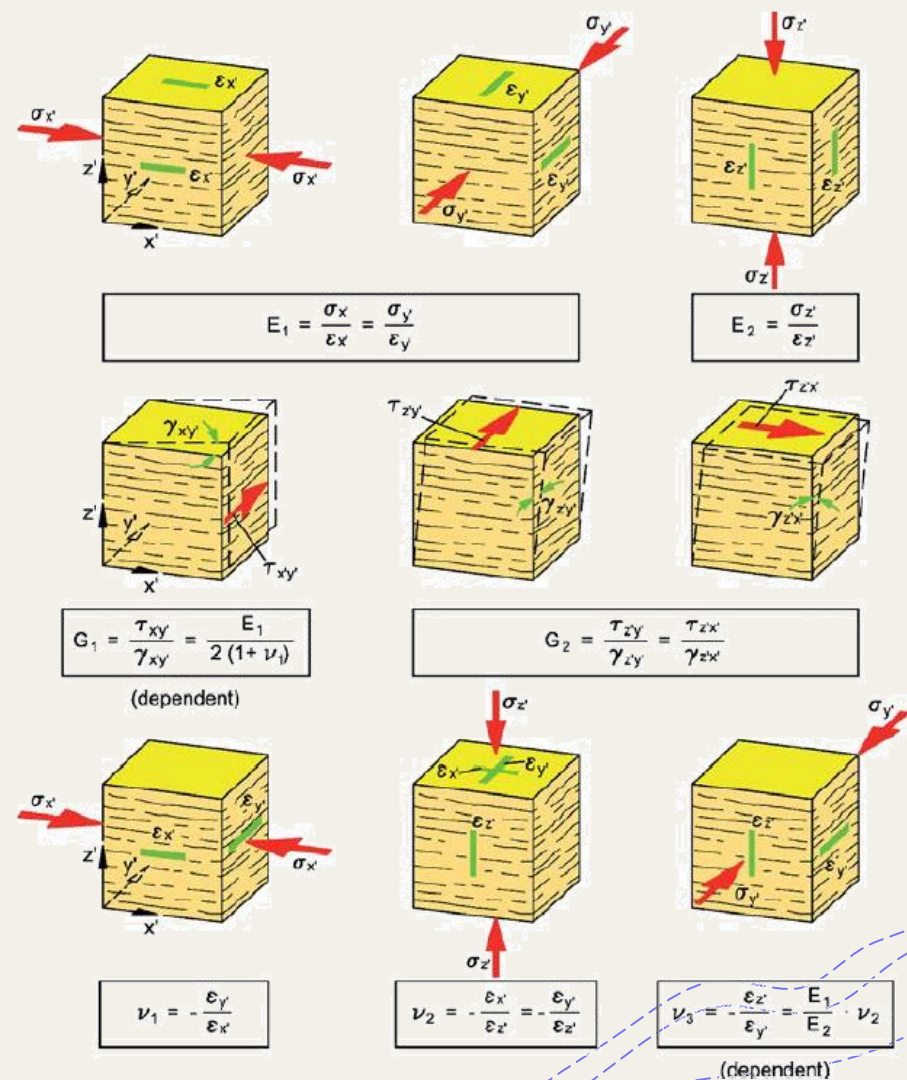


Fig. 7. Comparison of elastic modulus, uniaxial compressive strength and Brazilian tensile strength from laboratory tests (symbol), and those from bonded-particle DEM modeling (line). (a) Asan gneiss, (b) Boryeong shale, and (c) Yeoncheon schist.

5.2 岩體室內試驗

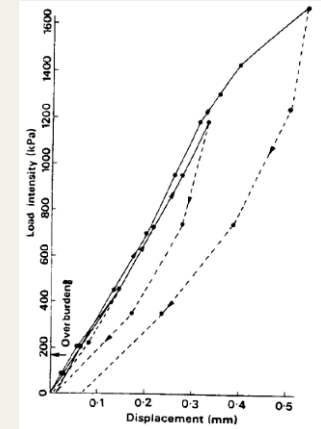
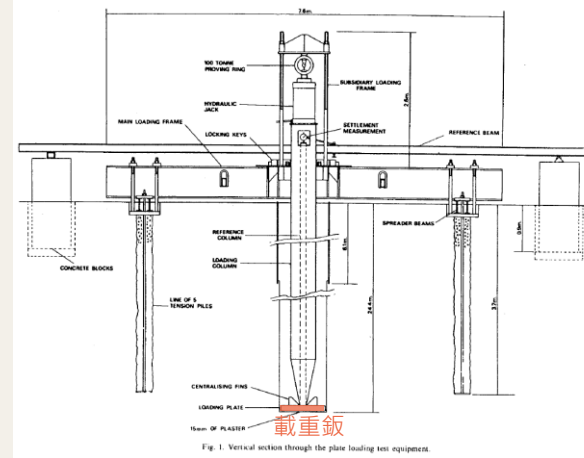
+ 橫向等向性材料

+ 左圖中有兩個參數相關(dependent)，獨立變數共5個 E_n 、 G_{ns} 、 ν_{sn} 、 E_s 、 ν_{st}



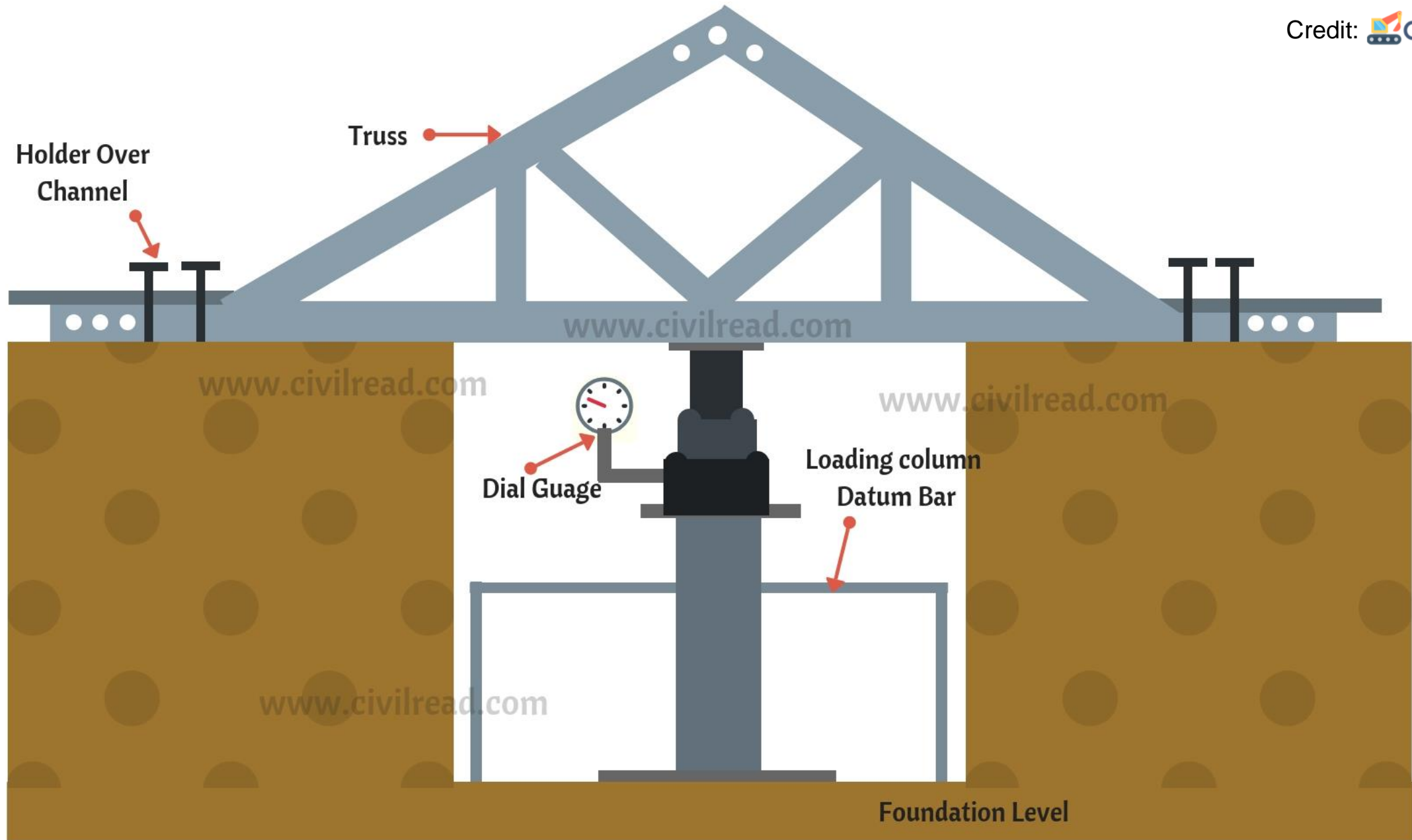
+ Plate bearing test 平板載重試驗

5.3 岩體現地試驗

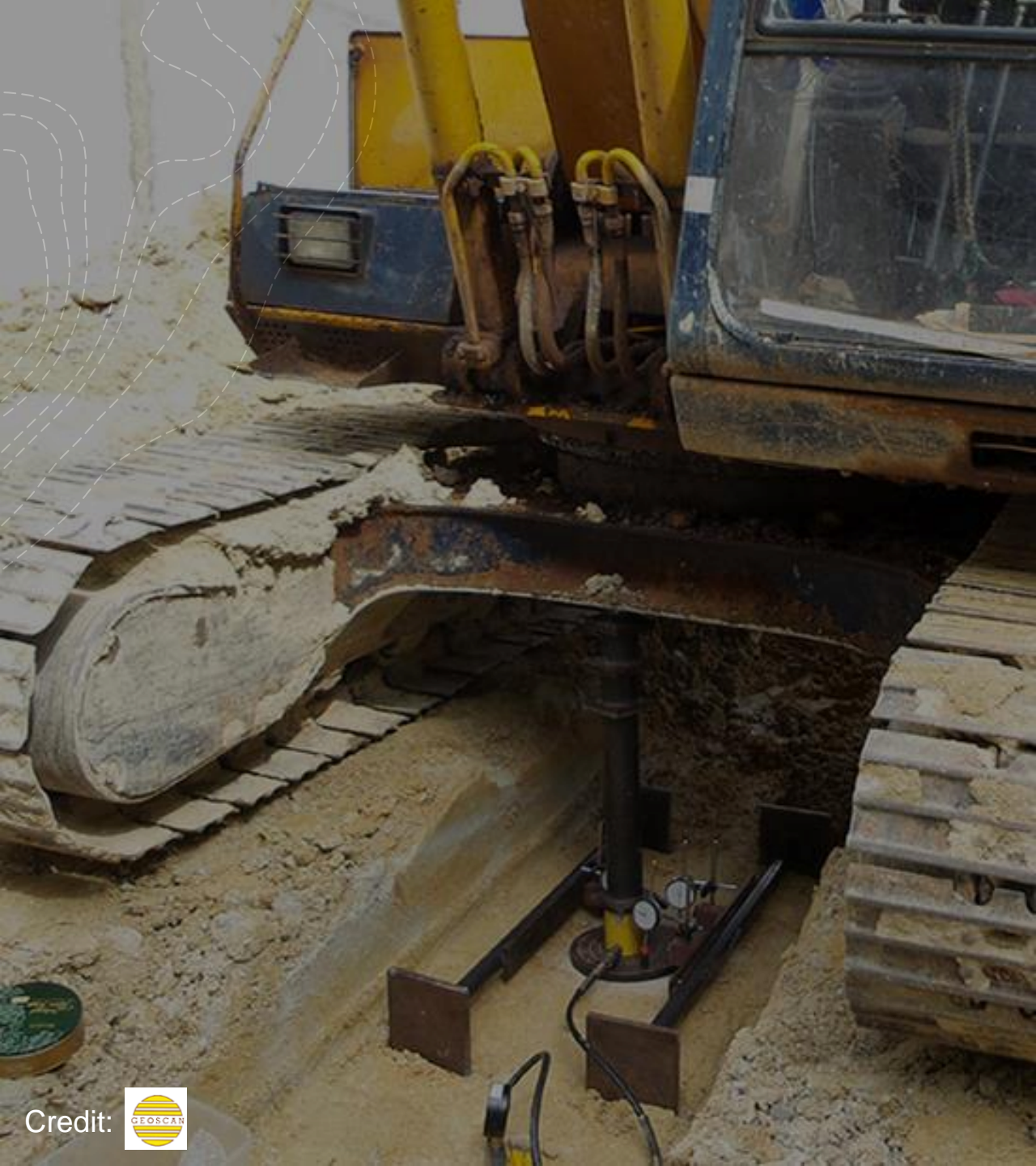


ISRM (1981)

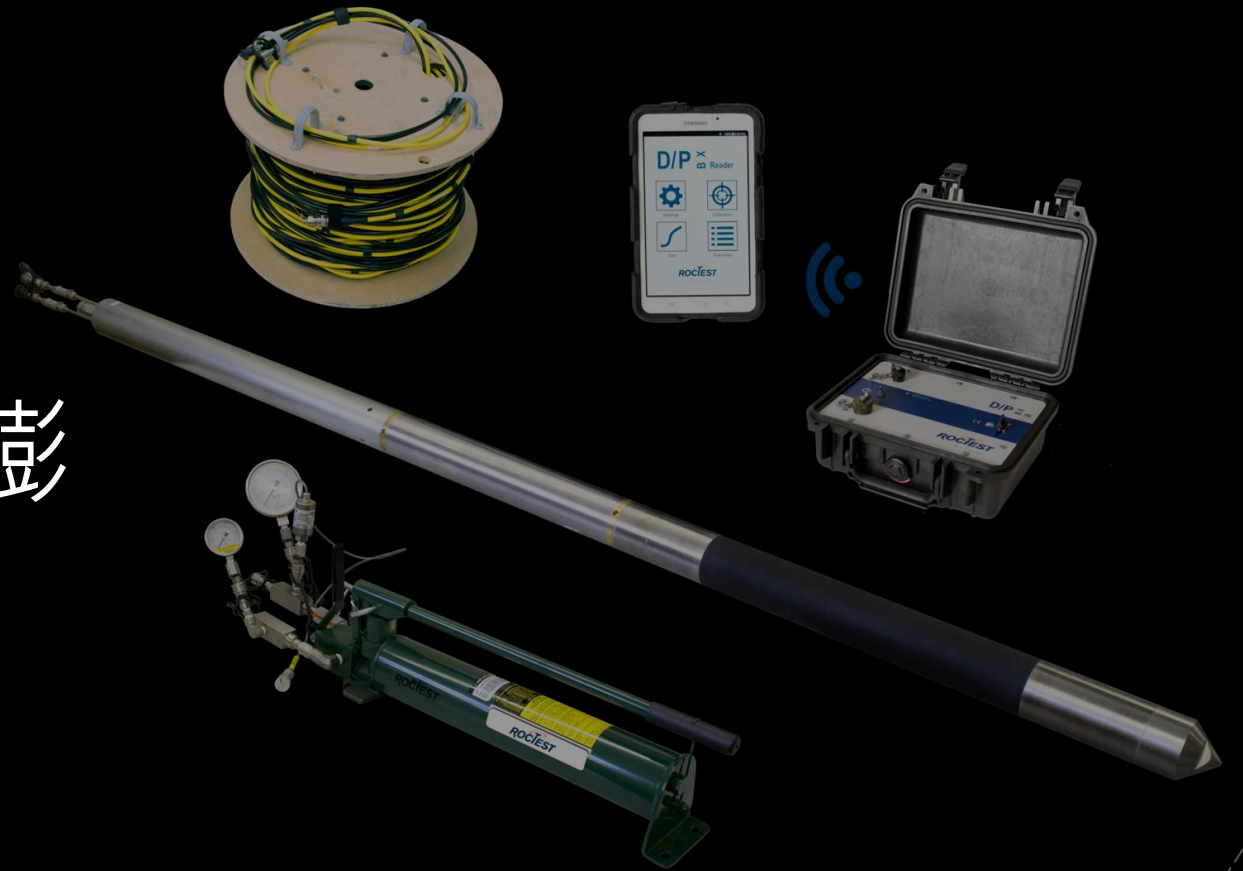
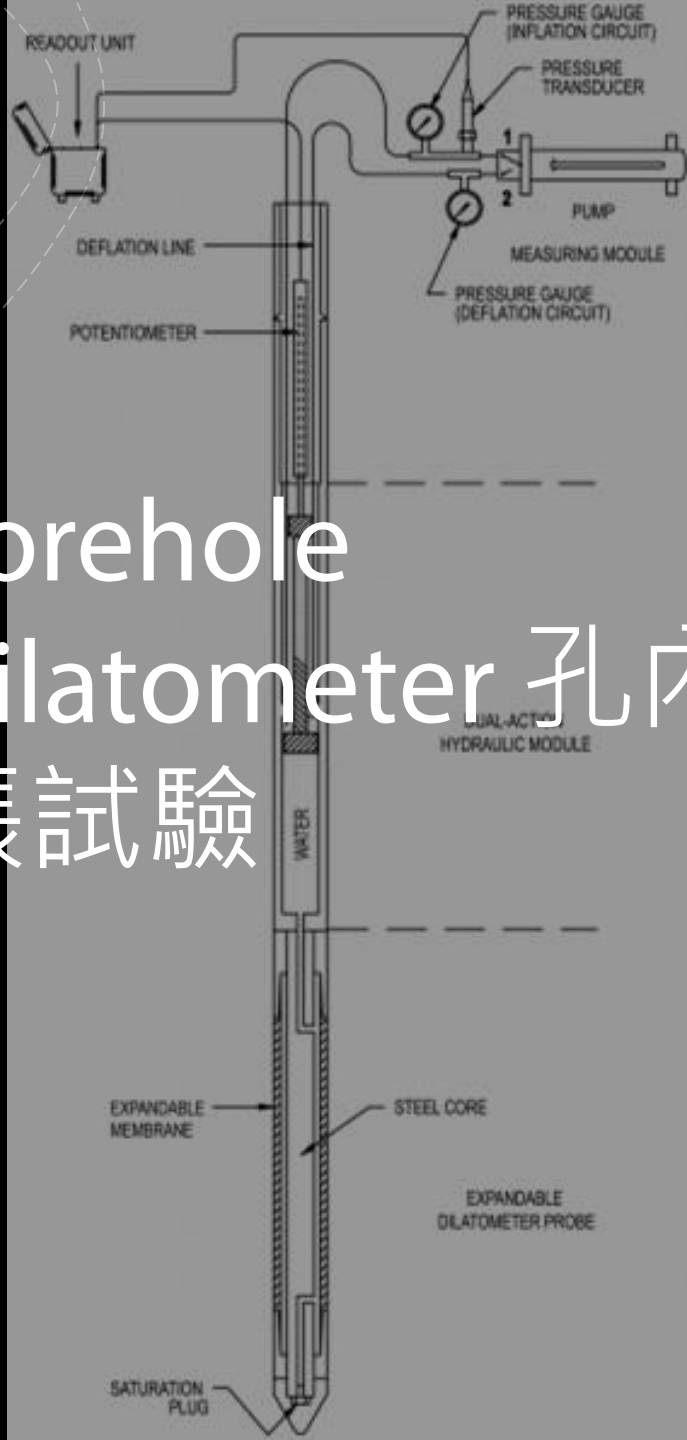




Reaction Truss Method - Plate Load Test



Borehole Dilatometer 孔內膨脹試驗



節理間距非常大

Calculation of deformability parameters of rock

12. (a) For any segment of the pressure displacement diagram (e.g. Fig. 7) and in rock with widely spaced joints [see 12(b) below], the corresponding secant dilatometric modulus E_d may be calculated as follows:

where:
$$E_d = (1 + \nu_R) D \frac{\Delta p_i}{\Delta D} \text{ (MPa)}$$

- Δp_i = pressure increment within the considered segment (MPa);
- ΔD = corresponding average change in drillhole diameter D (m);
- ν_R = Poisson's ratio of the rock mass.

節理間距很密,

岩體破碎

(b) If the test is performed in cracked rock, and if p_i exceeds about twice the average ground pressure p_0 around the drillhole, all existing radial cracks will open, and the equation of paragraph 12(a) is to be replaced by:

$$E_d = D \frac{p_i}{\Delta D} (1 + \nu_R) \left[(1 - \nu_R) \ln \left(\frac{p_i}{2p_0} \right) + 1 \right] \text{ (MPa)}$$

where:

- p_i = applied pressure (MPa), and
- ΔD = average increase of drillhole diameter (m), when pressure increases from zero to p_i .

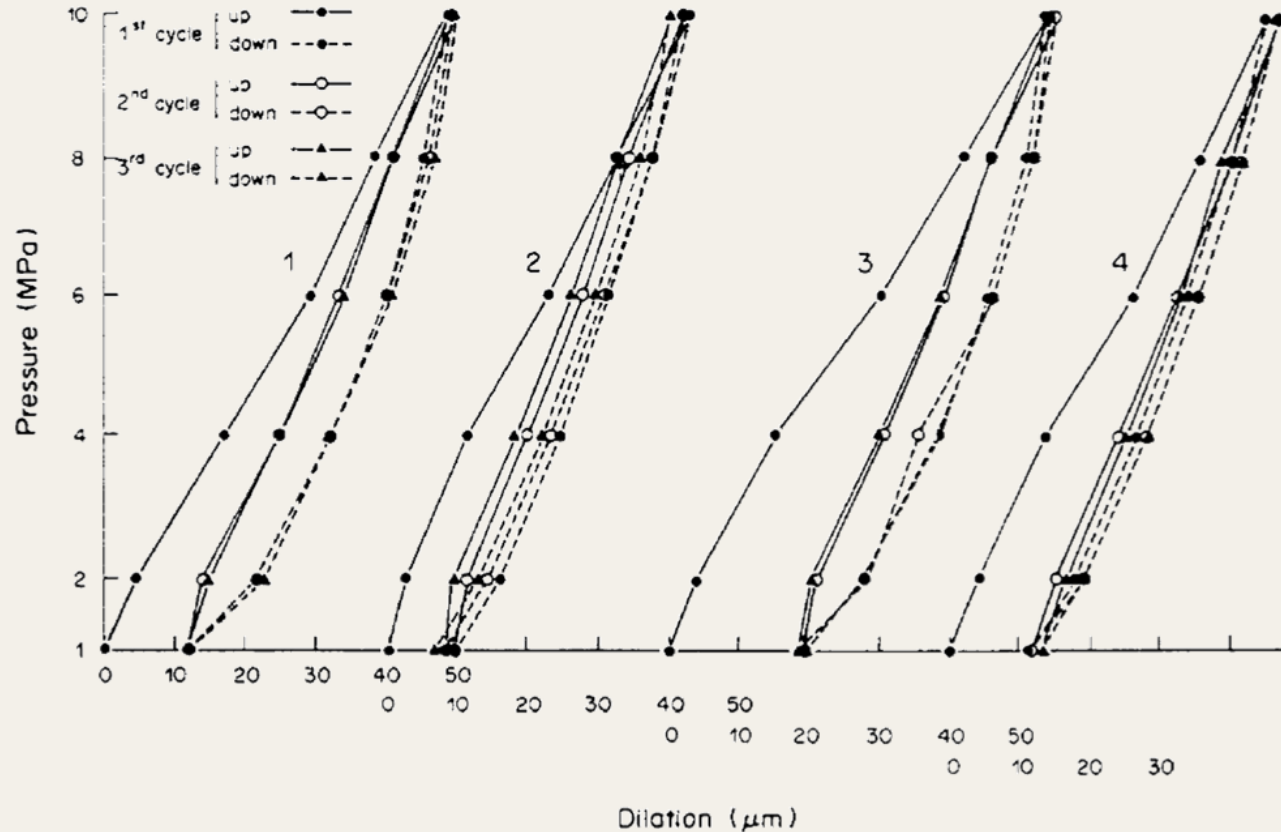
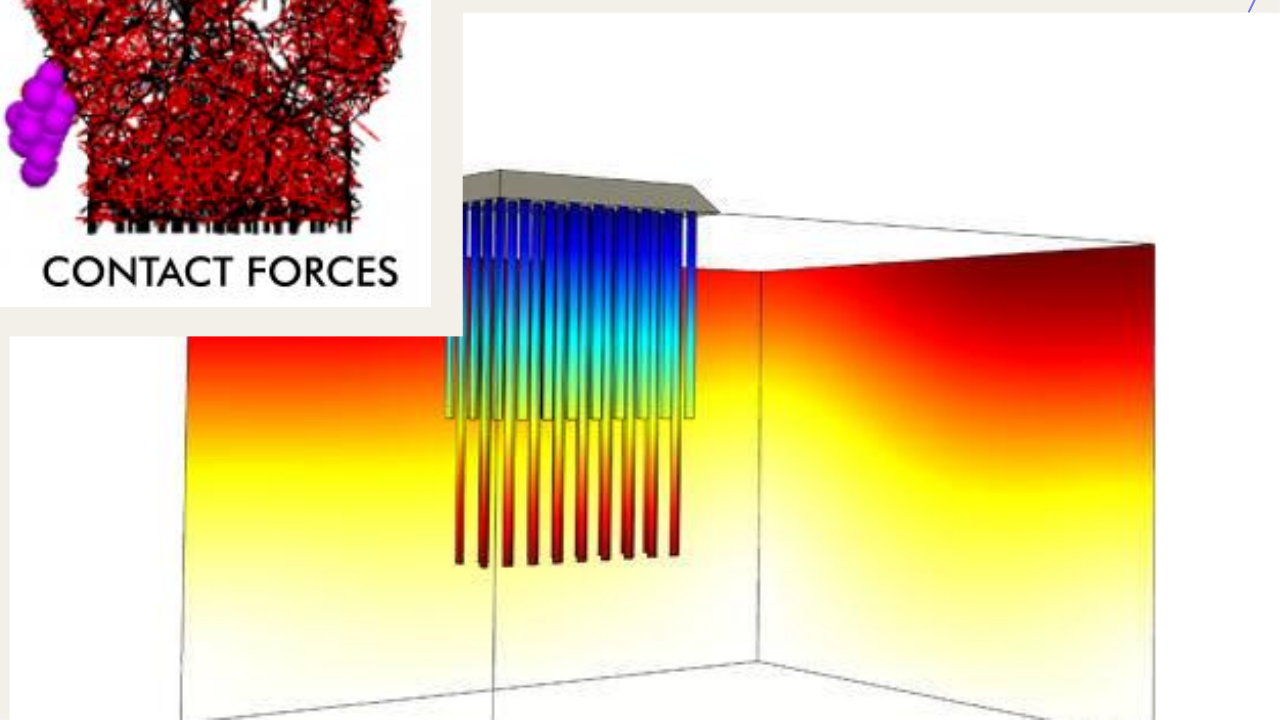
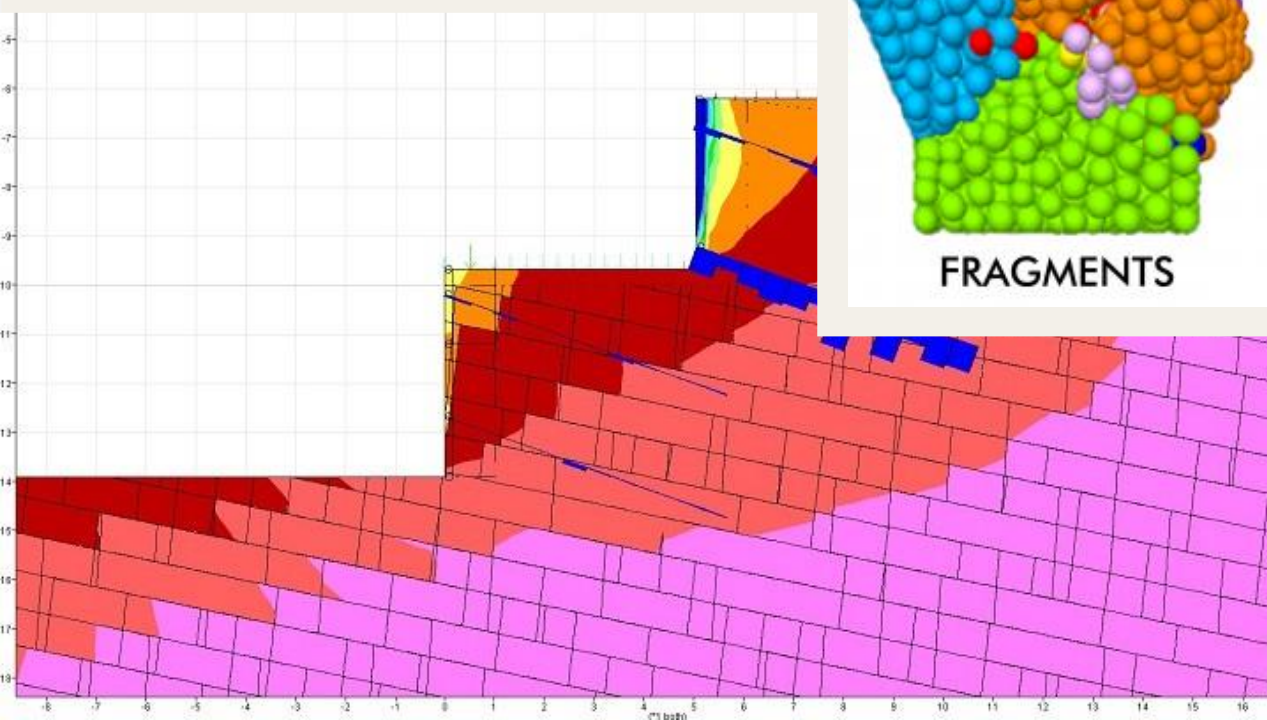
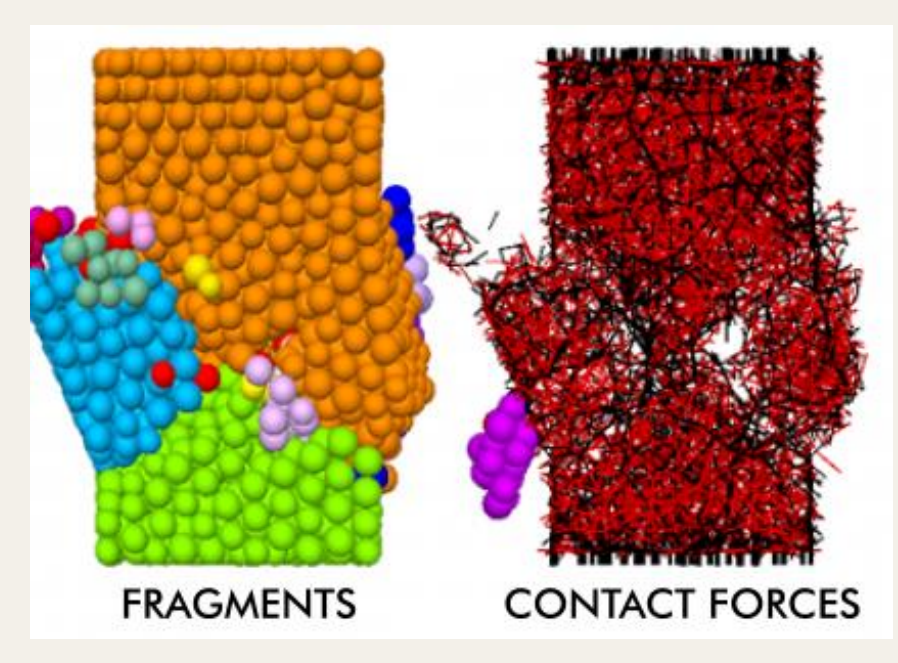
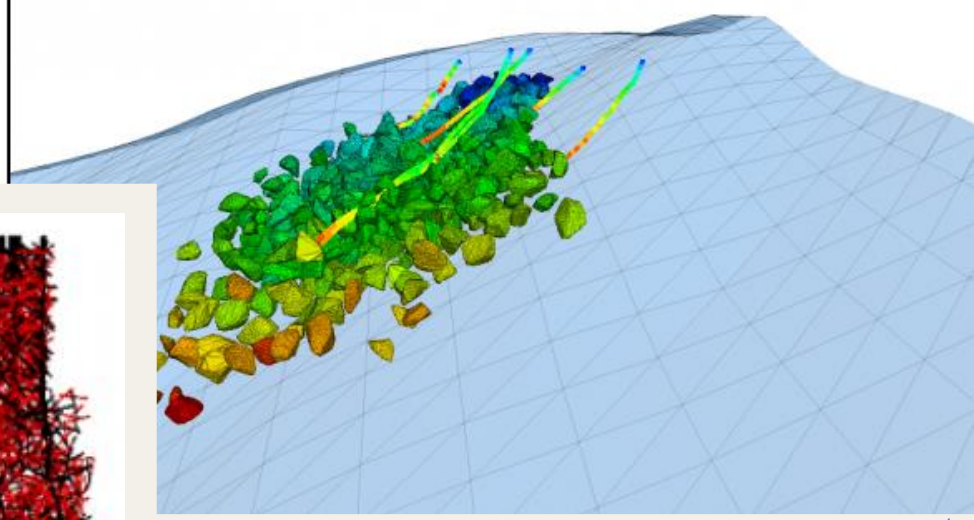
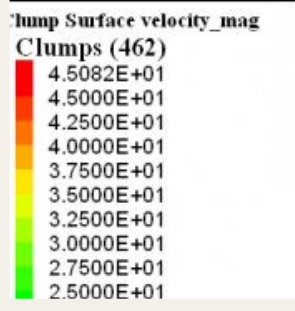
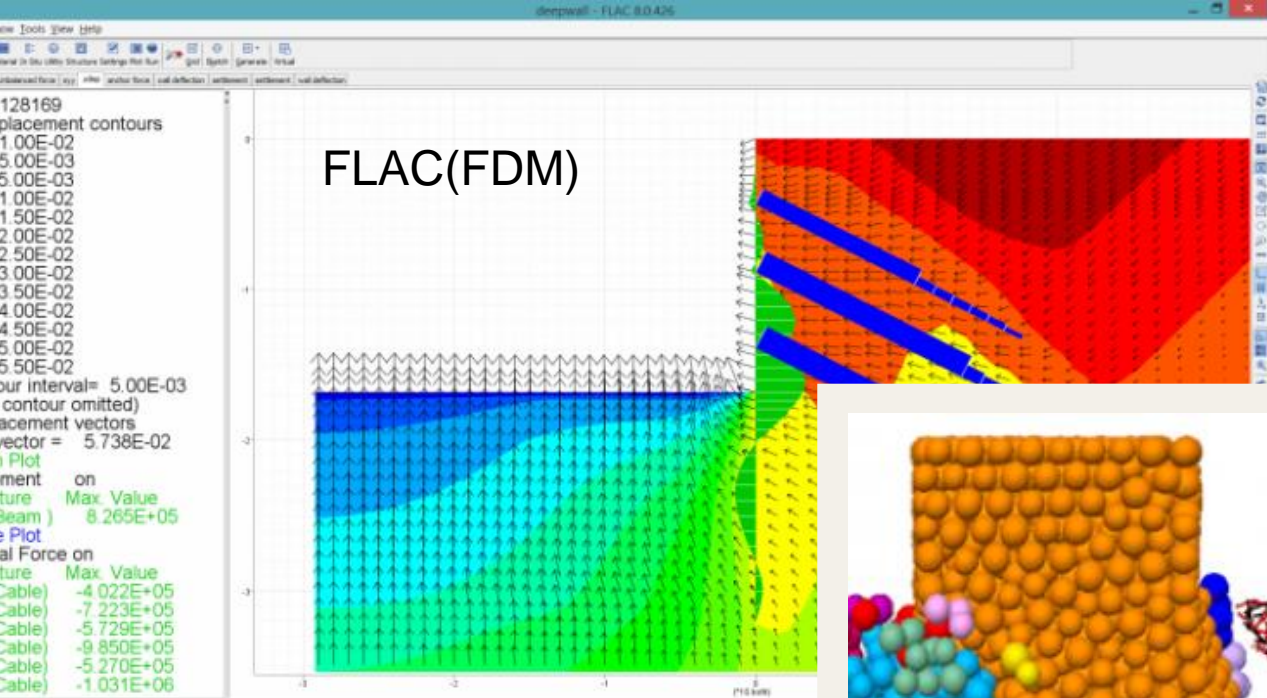


Fig. 7. Pressure-dilation curves, showing separate curves for each of four dilation-measuring transducers mounted in the same probe (LNEC dilatometer, [2, 20]).

5.4 岩體的數值模擬

FEA(Finite Element Analysis)

- + 有限元素法FEM(Finite Element Method), 如Abaqus, Plaxis, RS2, RS3...
- + 有限差分法FDM(Finite Difference Method), 如FLAC
- + 邊界元素法BEM(Boundary Element Method)
- + 離散元素法DEM(Distinct Element Method), 如UDEC, PFC2D, PFC3D...
- + 不連續變形分析DDA(Discontinuous Deformation Analysis)
- + 無網格法Mesh-free method
- + 混合(以上兩種或以上之分析)法Hybrid method



5.5 岩體分類法 參考第二章

+ 我國常見之岩體分類法包含：

+ 南非CSIR的Bieniawski之岩體評分法 (Rock Mass Rating, RMR)

+ 挪威NGI的Barton等人之Q法 (Q-system)

+ 台灣岩體分類法(台灣地區岩體分類系統, PCCR)

+ 坡體評分法 (Slope Mass Rating, SMR)

+ 其他，如美國Wickham等人提出之岩石構造評分法(Rock Structure Rating, RSR)